Photoinduced Electron Transfer in Clicked Ferrocene-BODIPY-Fullerene Conjugates

Jad Rabah, Anam Fatima, Hélène Fensterbank, Karen Wright, Anne Vallée, Maïssa Gueye, Gotard Burdzinski, Gilles Clavier, Fabien Miomandre, Julie Pham, et al.

Photoinduced electron transfer in clicked Ferrocene-BODIPY-Fullerene conjugates

Jad Rabah,[a#] Anam Fatima,[b#] Hélène Fensterbank,[a] Karen Wright,[a] Anne Vallée,[a] Maïssa Gueye,[a] Gotard Burdzinski,[c] Gilles Clavier,[d] Fabien Miomandre,[d] Julie Pham,[d] Michel Sliwa,[e] Rachel Méallet-Renault,[b] Karine Steenkeste,[b] Thomas Pino,[b] Minh-Huong Ha-Thi,[*b] Emmanuel Allard[*a]

[a] Université Paris-Saclay, UVSQ, CNRS, Institut Lavoisier de Versailles, 78 000, Versailles, France, e-mail: emmanuel.allard@uvsq.fr

[b] Université Paris-Saclay, CNRS, Institut des Sciences Moléculaires d'Orsay, 91 405, Orsay, France, e-mail: minh-huong.ha-thi@universite-paris-saclay.fr

[c] Fac Phys, Quantum Elec. Lab, Adam Mickiewicz Univ in Poznan, 61614 Poznan, Poland

[d] PPSM, Université Paris-Saclay, ENS Paris-Saclay, CNRS, 91190 Gif-sur-Yvette, France

[e] Université de Lille, CNRS, UMR 8516, Laboratoire de Spectroscopie pour les Interactions, la Réactivité et l'Environnement, 59 000 Lille, France.

[#]The two authors contributed equally to this work.

Abstract Text. Ferrocene-BODIPY (Fc-BDP) conjugates in which one or two ferrocene entities are linked to the β-positions of the BODIPY core by an ethynyl bridge have been developed. These derivatives were easily and efficiently grafted onto a dual-clickable fullerene platform using CuAAC reactions, leading to a clickable Fc-BDP-C_{60} triad and a clickable $[Fc]_2$-BDP-C_{60} tetrad which can be used for further derivatization with complex structures. Due to the extended π-conjugation and the presence of an intramolecular charge transfer band from Fc to BDP, all these conjugates display a broad absorption in the visible region, which is bathochromically shifted when two Fc are appended to the BDP core. Ultrafast multistep electron transfers leading to charge stabilization were demonstrated in the Fc-BDP-C_{60} triad and $[Fc]_2$-BDP-C_{60} tetrad by femtosecond transient absorption studies.

Keywords: Fullerenes, Boron dipyrromethenes, Ferrocene, Donor-acceptor systems, CuAAC reaction, electron transfer

Introduction

Since their discovery, fullerene C_{60} and its derivatives have led to many promising applications in the fields of life[1,2,3] and material sciences.[4,5,6,7,8] This scientific interest has continued to increase in recent years. This can be associated firstly with the unique physical and chemical properties displayed by fullerene C_{60} and its derivatives. In addition, significant progress has been made over the years in fullerene chemistry. Fullerene derivatives can be synthesized either by a direct approach[9,10] or by a post-functionalization route.[11] This latter strategy, using in particular click chemistry, has allowed the synthesis of sophisticated

structures that are difficult to access using the direct approach.[11] Among the large number of fullerene derivatives described in the literature, the class of Donor-C_{60} conjugates has emerged as one of the most important for applications related to solar energy conversion.[4-8] This can be explained by considering the outstanding acceptor properties and low reorganization energy in electron transfer processes displayed by fullerene C_{60}.

Among the different donors, also displaying light-harvesting properties, that have been linked to C_{60}, BODIPYs (4,4'-difluoro-4-bora-3a,4a-diaza-s-indacenes) have recently gained in importance. These chromophores have remarkable optical and chemical properties, including strong absorption in the visible region with molar absorbance approaching 10^5 $M^{-1}.cm^{-1}$ and fluorescence efficiencies close to 100%, with excellent photo-stability.[12] In addition, BODIPYs can be easily derivatized leading to a modulation of their optical and electrochemical properties.[12,13] Their association with C_{60} led to photo-induced energy and/or electron transfer processes in a large number of BODIPY-C_{60} conjugates, which have been exploited in various applications including solar energy conversion (mainly in artificial photosynthetic systems),[14,15,16,17,18,19,20,21,22,23] triplet-triplet annihilation up-conversion[24,25,26,27,28] and photocatalysis.[29] Most of these reported conjugates were prepared by functionalization of C_{60} with BODIPY derivatives in the final step (direct approach). One of the main drawbacks of this method remains the formation of undesired multi-adduct derivatives due to the multi-functional nature of fullerene, resulting in the loss of part of the BODIPY precursors, and the formation of the target assembly in only limited yields (up to 50%). Moreover, this strategy could be limiting in certain cases, in particular when it comes to combining BODIPY and C_{60} with more complex molecular structures such as inorganic compounds, polymers, dendrimers, peptides and biological systems.

For these reasons we have recently proposed a different strategy, based on a post-functionalization pathway using clickable fullerene building blocks that bear two different reactive centers. These derivatives were easily and efficiently functionalized with different BODIPY derivatives in yields greater than 85% using click reactions (thiol-maleimide or CuAAC).[30,31,32] In addition, these BODIPY-C_{60} conjugates have an available chemical functionality (free or protected alkyne) for further derivatisation with complex structures (*vide supra*). In all BODIPY-C_{60} dyads obtained by this method, a rapid photo-induced electron transfer from BODIPY to C_{60} was clearly demonstrated in conformers, with close proximity of the D and A moieties, and a short lifetime of the charge separated state. However, competitive photo-induced energy transfer processes were also observed within these dyads.[31,33]

In order to broaden the scope of the BODIPY-C_{60} conjugates using this strategy, we decided to attach additional redox entities such as ferrocene (Fc) to the BODIPY core, which should lead to a modification of the photophysical and photodynamic properties (*vide infra*) within the resulting assemblies. Surprisingly, despite the interesting features that could result from the association of these three entities, examples of Fc-BDP-C_{60} conjugates are scarce.[34,35,36] The main purpose of such assemblies, according to the authors, was to design efficient light-harvesting systems that could undergo a cascade multistep electron transfer process, resulting in the lengthening of the charge separated state lifetimes, as these properties are an important requirement for solar energy conversion applications. For example, Fukuzumi and co-workers reported the synthesis of two Fc-BDP-C_{60} triads with visible light-absorbing properties that could be extended to the NIR region for one of the triads.[34,35] In both assemblies, a cascade

PET (photoinduced electron transfer) process took place upon photoexcitation of the BODIPY leading to charge stabilization, with radical ion-pair lifetimes of 416 ps and 500 ps, respectively.[34, 35] Finally, Nemykin and co-workers reported the synthesis and characterization of NIR-absorbing Fc(s)-BDP-C_{60} conjugates.[36] In this case, an inefficient cascade electron transfer process was observed upon photoexcitation of the BODIPY of the assemblies.

In this article, we report the synthesis and characterization of a Fc-BODIPY-C_{60} triad and a $[Fc]_2$-BDP-C_{60} tetrad from a clickable fullerene core and azido-Fc-BODIPY derivatives. The fullerene building block, which was recently reported, carries two different reactive centers: an alkyne moiety on one side and a protected alkyne on the other.[32] For the azido-Fc-BODIPY conjugates, we chose structures in which one or two Fc entities are linked to the β-positions of the BODIPY core by an ethynyl bridge, which promotes good electronic communication between the redox centers. This type of assembly has already been reported[37,38] and displays interesting features for solar energy conversion applications: 1) wide absorption in the visible to the NIR region due to the increased π-conjugated system as well as the presence of a charge transfer band; 2) severely quenched fluorescence emission which could be attributed to photo-induced electron transfer from the Fc to the excited BODIPY upon irradiation. The occurrence of this process is key to the electron transfer cascade expected in the Fc-BODIPY-C_{60} conjugates presented in this article. These photo-induced electron transfer processes were investigated in these conjugates by steady-state and time-resolved spectroscopy techniques.

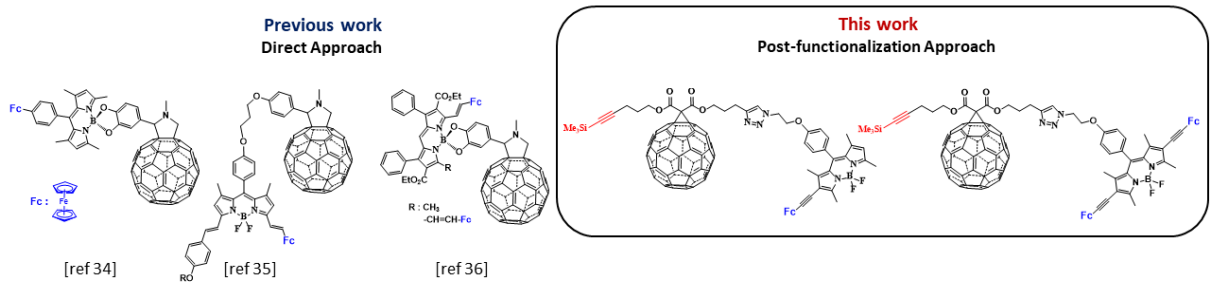

Figure 1. Fc-BDP-C_{60} conjugates previously described in the literature and those presented in this work.

Results and Discussion

Synthesis and Characterization

In order to functionalize the β–positions with Fc units, the starting BDP building block **1** was prepared *via* a three step one-pot approach (condensation, oxidation, and complexation) by reacting the commercially available hydroxyethoxybenzaldehyde and 2,4-dimethylpyrrole derivatives in DCM according to a procedure reported in the literature.[13] The resulting BDP starting material **1** was obtained in 40% yield in small scale reactions (~ 100 mg). Unfortunately, yields dropped to 20% when we attempted to produce this compound on a larger scale. Such reactions are known to be particularly low-yielding when using a β-unsubstituted pyrrole substrate, resulting in the formation of many side-products (confirmed by TLC) during the condensation reaction with the aldehyde derivative. Optimization of the reaction conditions by increasing the solvent volume and the reaction time eventually afforded a 40% yield on a gram scale (Scheme 1). Iodination of **1** under mild conditions using 1 equiv. or an excess of N-iodosuccinimide (NIS) in a mixture of DCM/DMF or DCM, led to the formation of the target

β-mono-iodo BDP **2** or β-bis-iodo BDP **3** precursors in 66% and 90% yields respectively (Scheme 1).[39-40]

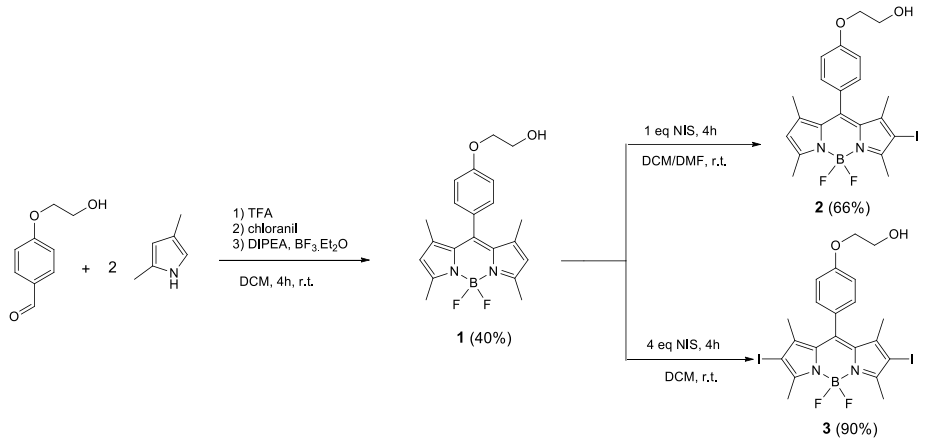

Scheme 1. Synthesis of the BDP **1** starting material and the β-iodo BDP precursors **2** and **3**.

The desired β-mono-ethynyl-Ferrocene BODIPY (Fc-BDP) **4** and β-bis-ethynyl-Ferrocene BODIPY ($[Fc]_2$-BDP) **6** were both obtained efficiently in 80% and 76% yields, by reacting the precursors **2** and **3** respectively with an excess of ethynylferrocene under Sonogashira cross coupling reaction conditions (Scheme 2).[37-38] Ferrocene-Bodipy azide derivatives **5** and **7** were then prepared using a one-pot procedure recently described.[32] Briefly, reaction of Fc-BDP **4** with NBS and PPh_3 in DCE at 0°C for one hour resulted in the complete consumption of the starting material **4**, accompanied by the formation of a new compound (monitored by TLC), namely the corresponding bromo-BDP intermediate. Then, the reaction of the latter derivative with NaN_3 (25% in H_2O) and two drops of Aliquat 336 at 80°C afforded the desired azido-Fc-BDP **5** in 50% yield after purification by column chromatography (Scheme 2). Following the same procedure, the target $[Fc]_2$-BDP azide conjugate **7** was successfully synthesized and isolated in 47% yield.

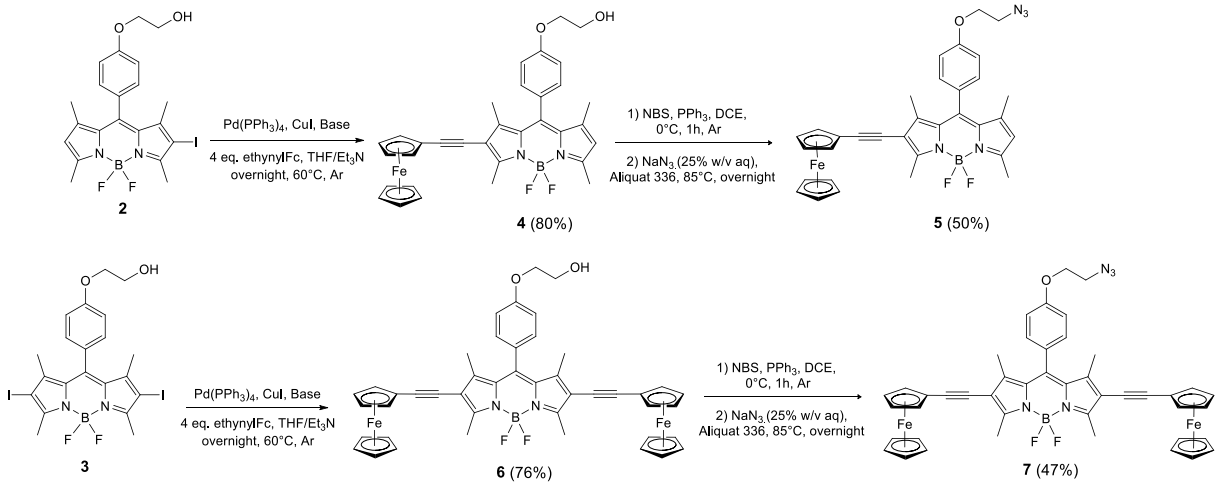

Scheme 2. Synthetic strategies for the formation of Fc-BDP azide derivatives **5** and **7**.

Finally, the azido-Fc-BDP precursors were grafted onto the clickable methanofullerene platform **8**, bearing on one side an alkyne and on the other a protected alkyne, under CuAAC conditions.[30, 32] Reaction of the azido-Fc-BDP derivative **5** with **8** in the presence of CuBr and

DIPEA in DCM yielded the target Fc-BDP-C_{60} triad **9** in 91% yield after purification by column chromatography (Scheme 3). Similarly, the reaction between **7** and **8** under the same conditions afforded the target $[Fc]_2$-BDP-C_{60} tetrad **10** in 77% yield (Scheme 3).

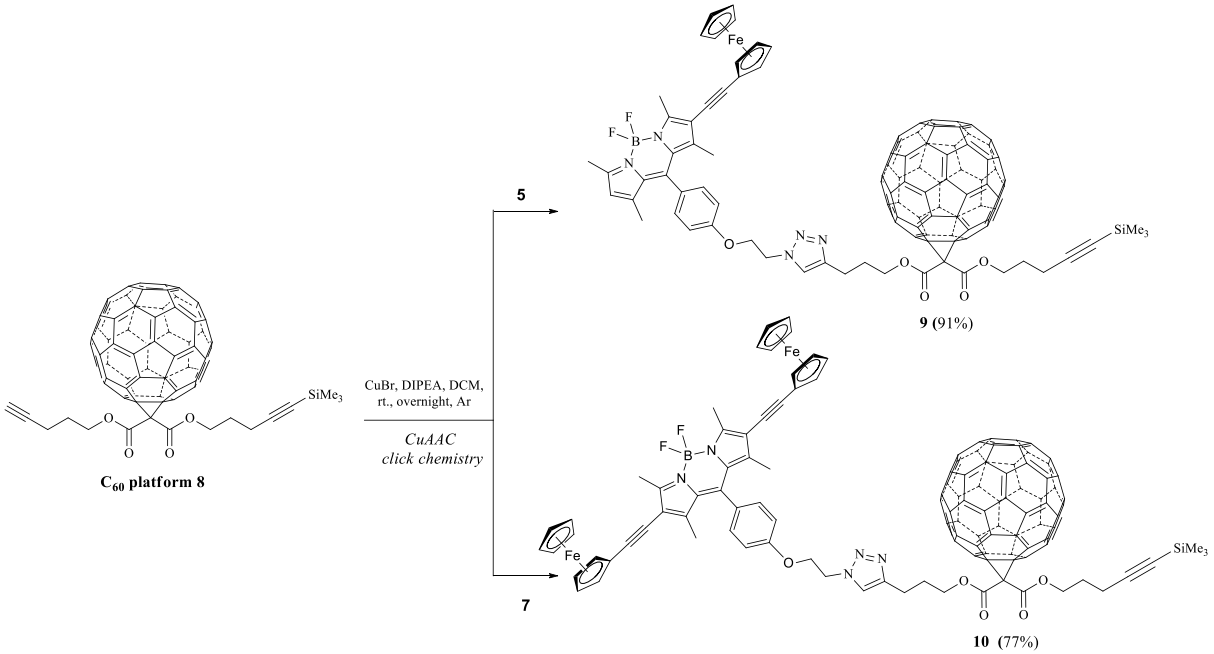

Scheme 3. Synthesis of Fc-BDP-C_{60} triad **9** and tetrad **10**.

All new compounds were fully characterized by NMR spectroscopy and by electrospray mass spectrometry; the recorded data were in accordance with the depicted structures (see supporting information). Examination of the ^{1}H NMR of the Fc-BDP-C_{60} triad **9** indicates the disappearance of the signal of the alkyne moiety while the peak of the TMS group remains intact as previously observed.[32] Furthermore, the typical singlet of the triazole unit appears as well as signals that correspond to the protons of the BDP and ferrocene moieties (Figure 2). The same features were observed for the $[Fc]_2$-BDP-C_{60} tetrad **10** (Figure S41).

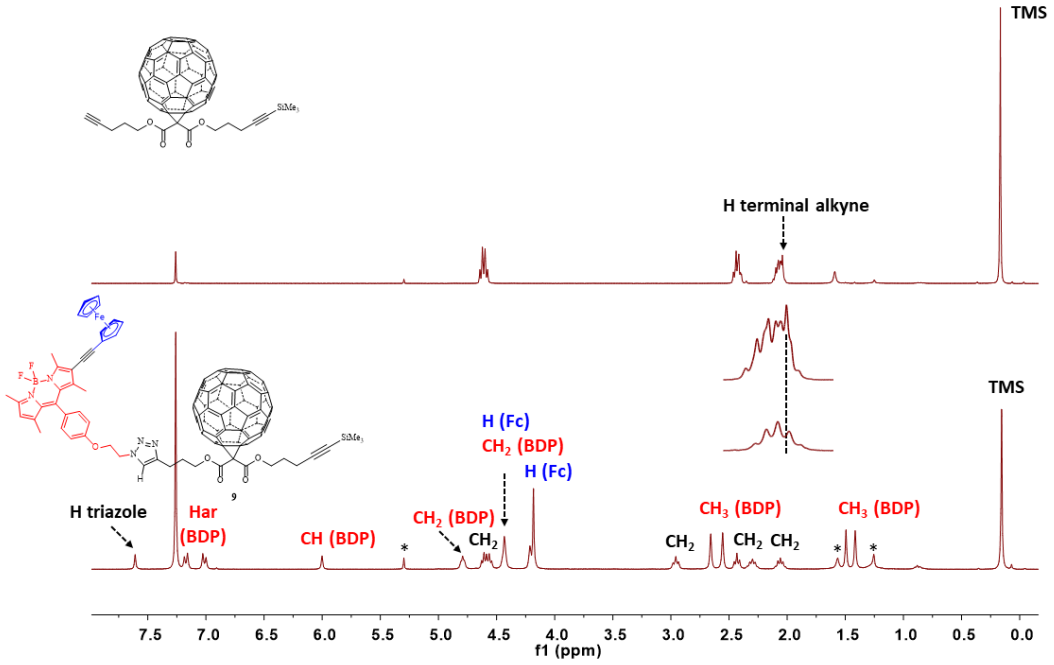

Figure 2. ^{1}H NMR spectrum recorded (300 MHz, $CDCl_3$, 25°C) for top: methanofullerene platform **8**; bottom: Fc-BDP-C_{60} triad **9**.

Absorption and Emission Spectroscopy

Absorption spectra of Fc-BDP-C_{60} triad **9** and $[Fc]_2$-BDP-C_{60} tetrad **10** recorded in benzonitrile along with their precursor conjugates (Fc-BDP **5** and $[Fc]_2$-BDP **7**) are shown in Figure 3a. The steady-state photophysical data are summarized in Table 1. The absorption spectrum of the dyad **5** with single conjugated ferrocene (Figure 3a) exhibits absorption bands at 534 and 390 nm, typical of the BODIPY-centered π-π* $S_0 \rightarrow S_1$ and $S_0 \rightarrow S_2$ transitions, respectively.[41] However, the 534 nm band is broadened as compared to typical BODIPY absorption due to the overlap of the intramolecular charge transfer (ICT) band from Fc to BDP.[37] In the triad **9**, additional absorption features were observed: a strong band at 330 nm and a small sharp band at 428 nm corresponding to the C_{60} platform (Figure 3a, Figure S51).[42] The absorption of the Fc moiety gives a negligible contribution due to its low molar absorption coefficient (61 M^{-1} cm^{-1} at 322 nm).[43]

Compared to Fc-BDP dyad **5**, both $S_0 \rightarrow S_1$ and $S_0 \rightarrow S_2$ transition bands of $[Fc]_2$-BDP triad **7** are bathochromically shifted (by 46 nm and 15 nm respectively) owing to the more significant extended π-conjugation when the second ferrocene was introduced to the Fc-BDP core. In line with this, the $[Fc]_2$-BDP-C_{60} tetrad **10** shows similar red-shifted $S_0 \rightarrow S_1$ transition bands as compared to that of Fc-BDP-C_{60} triad **9** (46 nm, Figure 3a). Moreover, the $S_0 \rightarrow S_1$ bands of $[Fc]_2$-BDP triad **7** and $[Fc]_2$-BDP-C_{60} tetrad **10** are comparatively broader than in Fc-BDP **5** and Fc-BDP-C_{60} triad **9** compounds due to an additional ICT between the second Fc donor and the BDP acceptor. These results demonstrate the robust electronic interaction between the BDP and Fc entities, which is accentuated after the BDP core was modified to include the two ferrocene donor units.

Compared to typical BODIPY fluorophores, similar emission spectra with the same maxima at 555 nm were observed for the Fc-BDP **5** dyad and its corresponding fullerene triad (Fc-BDP-

C_{60} **9**), but the corresponding fluorescence quantum yields are very weak (2.2 and 1.4%, respectively) (Figure 3b). This is attributed to the photoinduced processes taking place in the excited state of BDP in the presence of the Fc and C_{60} moieties. In the case of bis-ferrocene substituted analogs $[Fc]_2$-BDP **7** and $[Fc]_2$-BDP-C_{60} tetrad **10**, emission quenching was so strong that no emission band was detected.

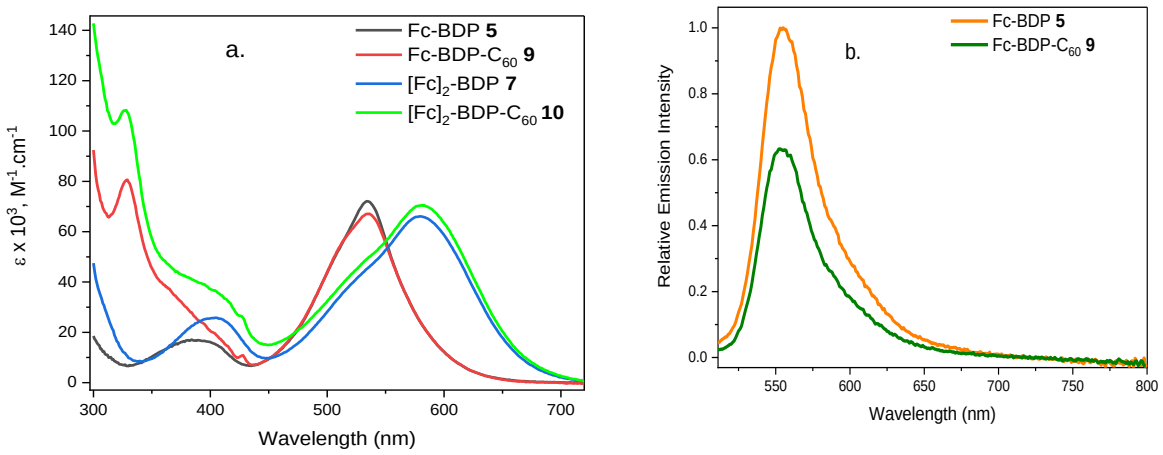

Figure 3. Steady-state (a) absorption spectra of Fc-BDP-C_{60} triad **9** and $[Fc]_2$-BDP-C_{60} tetrad **10** conjugates along with the references Fc-BDP **5** and $[Fc]_2$-BDP **7**, and (b) emission spectra of Fc-BDP dyad **5** and the corresponding C_{60} triad **9** recorded in benzonitrile (λ_{exc} = 500 nm).

Time-resolved emission

In order to gain more insight into the quenching of the BDP moiety by Fc and C_{60}, time-correlated single photon counting (TCSPC) measurements were performed in benzonitrile. The fluorescence decays of the Fc-BDP dyad **5** and Fc-BDP-C_{60} triad **9** are shown in Figure 4.

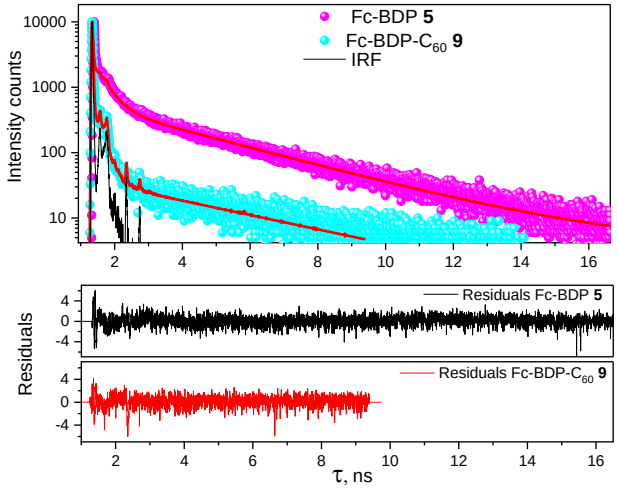

Figure 4. Fluorescence decay of Fc-BDP dyad **5** (λ_{exc} = 495 nm, λ_{em} = 555 nm) and Fc-BDP-C_{60} triad **9** (λ_{exc} = 495 nm, λ_{em} = 555 nm) in benzonitrile.

A fluorescence lifetime of several nanoseconds was measured for a similar BODIPY in benzonitrile.[31] However, the decays of Fc-BDP dyad **5** and Fc-BDP-C_{60} triad **9** were satisfactorily fitted with three exponentials, yielding one very short principal time-constant of several picoseconds (> 96%) which is below the instrumental response function. This short component indicates some rapid electron and/or energy transfer events taking place in the excited state of the BODIPY moiety. Further, the greater contribution of this short component in the fluorescence decay of Fc-BDP-C_{60} triad **9** as compared to that of Fc-BDP dyad **5**, which is in line with the lower fluorescence quantum yield of the triad **9**, indicates additional deactivation pathways due to the added C_{60} moiety in the triad. Photoinduced processes will be further elucidated by femtosecond transient absorption. Table 1 summarizes the time-constants obtained by TCSPC.

Table 1 Absorption and emission characteristics of Fc-BDP **5** and $[Fc]_2$-BDP **7** conjugates along with Fc-BDP-C_{60} triad **9** and $[Fc]_2$-BDP-C_{60} tetrad **10** in benzonitrile.

Compound	**λ_{abs}, nm** **(ε, $M^{-1}cm^{-1}$)**	**λ_{em}, nm**	**Φ_F, %**	**τ, ns** **(amplitude, wt.%)**
Fc-BDP 5 [a]	390 (17 200), 534 (71 700)	555	2.2	0.013 (96%), 0.330 (3.04%), 3.0 (0.6%)
Fc-BDP-C_{60} 9 [a]	328 (80 200), 534 (67 100)	555	1.4	0.009 (99.8%), 0.184 (0.18%), 3.0 (0.01%)
$[Fc]_2$-BDP 7	405 (26 500), 580 (66 200)	--	--	--
$[Fc]_2$-BDP-C_{60} 10	328 (108 400), 580 (70 100)	--	--	--

Φ_F : Fluorescence quantum yield with 10 % error, Fluorescence lifetimes (contribution in %) with an error of ± 40 ps [a] λ_{exc} = 495 nm, λ_{em}= 555 nm, quantum yield measurement of the BODIPY moiety with Rhodamine 6G used as standard (λ_{exc} = 495 nm, ϕ = 95% in ethanol)

Electrochemical and Spectroelectrochemical studies

Electrochemical Studies

The electrochemical investigations on reference ethynylphenyl BODIPY compounds (**11** and **12**, see supporting information for their synthesis and characterization), Ferrocene-BODIPY conjugates (**4** and **6**), methanofullerene platform (**8**) and Ferrocene-BODIPY-C_{60} assemblies (**9** and **10**) were conducted by cyclic voltammetry (CV). All experiments were performed in a standard three-compartment electrochemical cell under argon atmosphere at room temperature in anhydrous dichloromethane solutions using tetra-*n*-butylammonium hexafluorophosphate ($TBAPF_6$) as a supporting electrolyte, and ferrocene (Fc) as an internal reference. The recorded cyclic voltammograms of all compounds are displayed in Figures 5 and

6. The half-wave potentials (V *vs* Fc^+/Fc) of the reference and target compounds are shown in Table 2.

Reference molecules **11** and **12** bearing either one or two ethynylphenyl appendages give an irreversible oxidation process attributed to the formation of the BDP π-radical cation ($BDP^{+\bullet}$), at nearly identical potentials (+0.77 V *vs* Fc^+/Fc for **11** and **12**) in comparison with unsubstituted BDP (+0.73 V *vs* Fc^+/Fc).[44] In the cathodic region, a reversible one-electron reduction at -1.46 V *vs* Fc^+/Fc attributed to the formation of the BDP π-radical anion ($BDP^{\bullet-}$) is observed for both compounds. In addition, the presence of the ethynylphenyl moities resulted in the increase of the potentials in comparison with the unsubstituted BDP (-1.70 V vs *vs* Fc^+/Fc),[44] rendering these reference derivatives more easily reduced.

The Fc-BDP **4** and $[Fc]_2$-BDP **6** each exhibit similar behavior in the cathodic region but to a lesser extent with a reversible one-electron reduction process at -1.60 V and -1.55 V *vs* Fc^+/Fc, respectively, corresponding to the formation of the $BDP^{\bullet-}$ (Figure 5, Table 2). In the anodic region, both compounds reveal a reversible as well as an irreversible one-electron oxidation (E^1_{ox} = 0.06-0.08 V and E^2_{ox} = 0.85-0.88 V *vs* Fc^+/Fc) corresponding to the formation of the ferrocenium cation Fc^+ and $BDP^{+\bullet}$ respectively. The anodically-shifted potential values of the ferrocenyl entities within the conjugates **4** and **6**, in comparison with free ferrocene (E^1_{ox} = 0.00 V), can be assigned to the electronic communication between the Fc donor(s) and BDP acceptor as previously reported.[38] The oxidation potentials of the $BDP^{+\bullet}$ species formed in compounds **4** and **6** are remarkably shifted to positive potential by 100 mV with respect to the reference molecules (Figure 5, table 2). Such behavior can be explained by the strong coulombic repulsion between the generated positive charge on the BDP backbone and the oxidized Fc^+ species. These electrochemical findings are in accordance with those reported in the literature for very similar structures.[38]

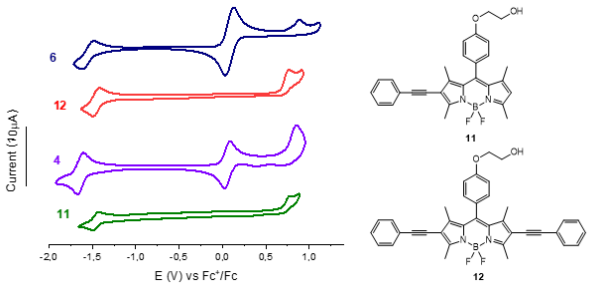

Figure 5. Cyclic voltammograms of the β-substituted BDP assemblies **4 (purple), 6 (blue), 11 (green)** and **12 (red)** in anhydrous and oxygen-free DCM, 0.1M of *n*-Bu_4NPF_6, pseudo-reference electrode: Ag wire, working electrode: Pt, auxiliary electrode: Pt, scanning rate: 100mV.s^{-1}.

The CVs recorded for methanofullerene platform **8** and Ferrocene-BODIPY-C_{60} assemblies **9** and **10** are displayed in Figure 6. The Fc-BDP-C_{60} triad **9** exhibited a reversible one-electron oxidation at 0.18 V (*vs* Fc^+/Fc) and an irreversible one-electron oxidation at 0.88 V (*vs* Fc^+/Fc) corresponding to the formation of Fc^+ and $BDP^{+\bullet}$ species, respectively. In the cathodic region, the CV displays two reversible reductions waves at -1.03 and -1.41 V (*vs* Fc^+/Fc). By comparison with the reduction potentials of those of the platform **8**, these two waves are undoubtedly attributed to the formation of $C_{60}^{\bullet-}$ and C_{60}^{2-} species, respectively. The reduction

of the BDP was not further investigated due to the instability of the methanofullerene moiety after several reduction processes, known as the retro Bingel-reaction.[32] Regarding the $[Fc]_2$-BDP-C_{60} tetrad **10**, the CV displayed reversible two-electron oxidation of the Fc units into $(Fc^+)_2$ in the anodic region, also at 0.14 V (*vs* Fc^+/Fc), whereas the oxidation of the BDP entity into the $BDP^{+\bullet}$ radical cation was not well-defined. In the cathodic region, two reduction waves appeared at -1.01 and -1.43 V (*vs* Fc^+/Fc). The first wave is attributed to the formation of fullerene radical anion $C_{60}^{\bullet-}$, while the second quasi-reversible signature could be assigned to two overlapping reductions corresponding to the dianion C_{60}^{2-} and $BDP^{\bullet-}$ species.

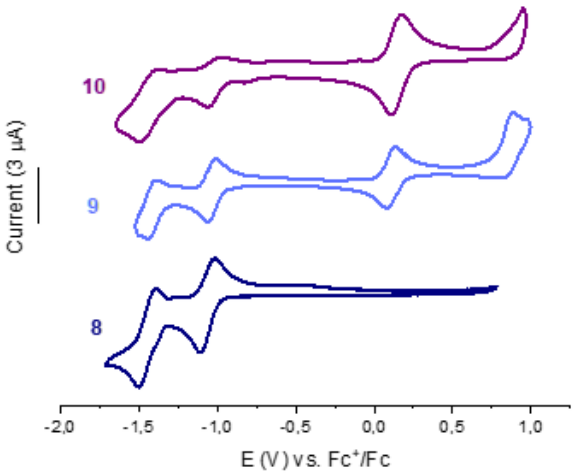

Figure 6. Cyclic voltammograms of the methanofullerene platform **8** (**navy blue**), Ferrocene-BODIPY-C_{60} assemblies **9 (blue)** and **10 (purple)** in anhydrous and oxygen-free DCM, 0.1M of *n*-Bu_4NPF_6, pseudo-reference electrode: Ag wire, working electrode: Pt, auxiliary electrode: Pt, scanning rate: 100 $mV.s^{-1}$.

Table 2. Electrochemical Half-Wave Potentials (V *vs* Fc^+/Fc) of ethynylphenyl BODIPY compounds **11** and **12**, Ferrocene-BODIPY conjugates **4** and **6**, methanofullerene platform **8** and Ferrocene-BODIPY-C_{60} assemblies **9** and **10**.

Compound	**Potential (V vs. Fc^+/Fc)**				
	$BDP^{0/+}$	$Fc^{0/+}$	$C_{60}^{0/-}$	$C_{60}^{-/2-}$	$BDP^{0/-}$
11	+0.77	-	-	-	-1.46
12	+0.77	-	-	-	-1.46
4	+0.85	+0.06	-	-	-1.60
6	+0.88	+0.08	-	-	-1.55
8			-1.06	-1.44	
9	+0.88	+0.18	-1.03	-1.41	-
10	--[a]	+0.14	-1.01	-1.43	-1.43

[a] wave not well-defined

UV-vis-NIR Spectroelectrochemistry

The BDP radical anion signature in the UV-Visible region was obtained by recording the spectral changes in the $[Fc]_2$-BDP triad **7** at varying reduction potentials (-0.7 to -1.2 V) leading to one-electron reduction of the BDP unit. The differencial spectroelectrochemical (SEC) spectra (Figure 7) show a sharp band at 550 nm accompanied by a small absorption band at 440 nm corresponding to the absorption of the reduced state while a negative band at 600 nm corresponds to the depletion of the electronic ground state. Similar spectral changes with positive absorption bands at 370 and 527 nm accompanied by a negative band at 570 nm were obtained for the Fc-BDP **5** dyad (see supporting information, Figure S52).

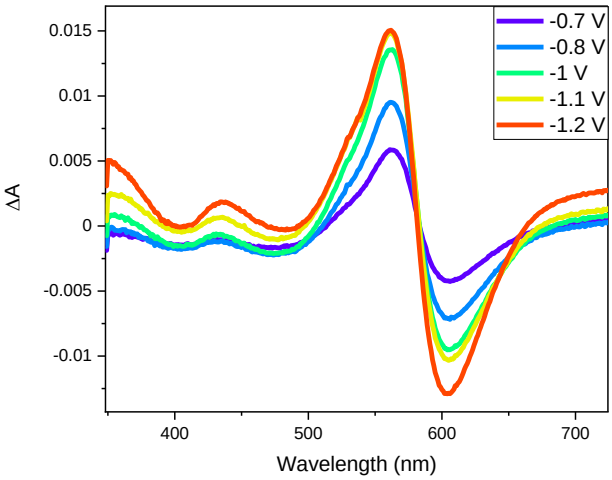

Figure 7. Spectroelectrochemical differential spectra relative to the neutral state of one electron reduced BDP in $[Fc]_2$-BDP triad **7** (10 µM) in the presence of 0.1 M $TBAPF_6$ in dichloromethane under different potentials.

Transient Absorption Studies

Femtosecond TA spectra were recorded to investigate the relaxation pathway in the Fc-BDP conjugates and their corresponding fullerene triad and tetrad in benzonitrile by selectively exciting the BDP unit (λ_{exc} = 580 nm).

i. *$[Fc]_2$-BDP triad* **7**

Femtosecond transient absorption spectra in the UV-Vis-NIR region of $[Fc]_2$-BDP triad **7** were recorded in argon-saturated benzonitrile and are shown in Figure 8. For clarity, the spectra are presented in four different time windows. The first time window [-0.15 to 0.2 ps] depicts the appearance of positive bands at *ca.* 350 and 440 nm in the UV-visible region and a broad absorption band in the NIR, accompanied by a negative absorption band centered at *ca.* 600 nm. The positive bands are attributed to the absorption of ^{1}BDP* while the negative TA band corresponds to the ground state depletion of BDP (inverted ground state absorption spectrum is added in the first time panel for comparison, grey curve in Figure 8 a).[33] From 0.2 to 3 ps, the ^{1}BDP* bands in the visible as well as the NIR regions decay in the same time as the appearance of a new positive TA band at 550 nm, and a broad absorption band centered at about 1100 nm

in the NIR. These spectral features can be attributed to an electron transfer from Fc to ^{1}BDP* to form a charge separated state Fc$^{\cdot+}$-BDP$^{\cdot-}$. The SEC spectrum provides a good overlap with the femtosecond TA spectra of the triad (black curve in panel b. of Figure 8). In the 3-50 ps time window, the TA bands corresponding to the BDP radical anion (440, 550 and 1100 nm) decay to simultaneously form two new TA bands at 450 and 650 nm. These latter bands can be attributed to the triplet excited state localized on BDP.[34] It implies that the Fc$^{\cdot+}$-BDP$^{\cdot-}$ ion pair recombines to populate the triplet state of the triad ^{3}**7***. It is worth noting that the charge separated state Fc$^{\cdot+}$-BDP$^{\cdot-}$ (1.68 eV) can populate ^{3}BDP* (1.55 eV)[45], ^{3}Fc* (1.16 eV)[35] or decay to the ground state. In the last time window, the decay of the triplet state restores the baseline and no transient signature was observed by complementary nanosecond transient absorption measurements. This rapid decay of the triplet state of the triad **7** as compared to that of a triplet state localized on a BODIPY[28] is likely due to the presence of the conjugated ferrocene moiety. This behavior was reported by Liu and coworkers for a similar ferrocene-BODIPY dyad.[35]

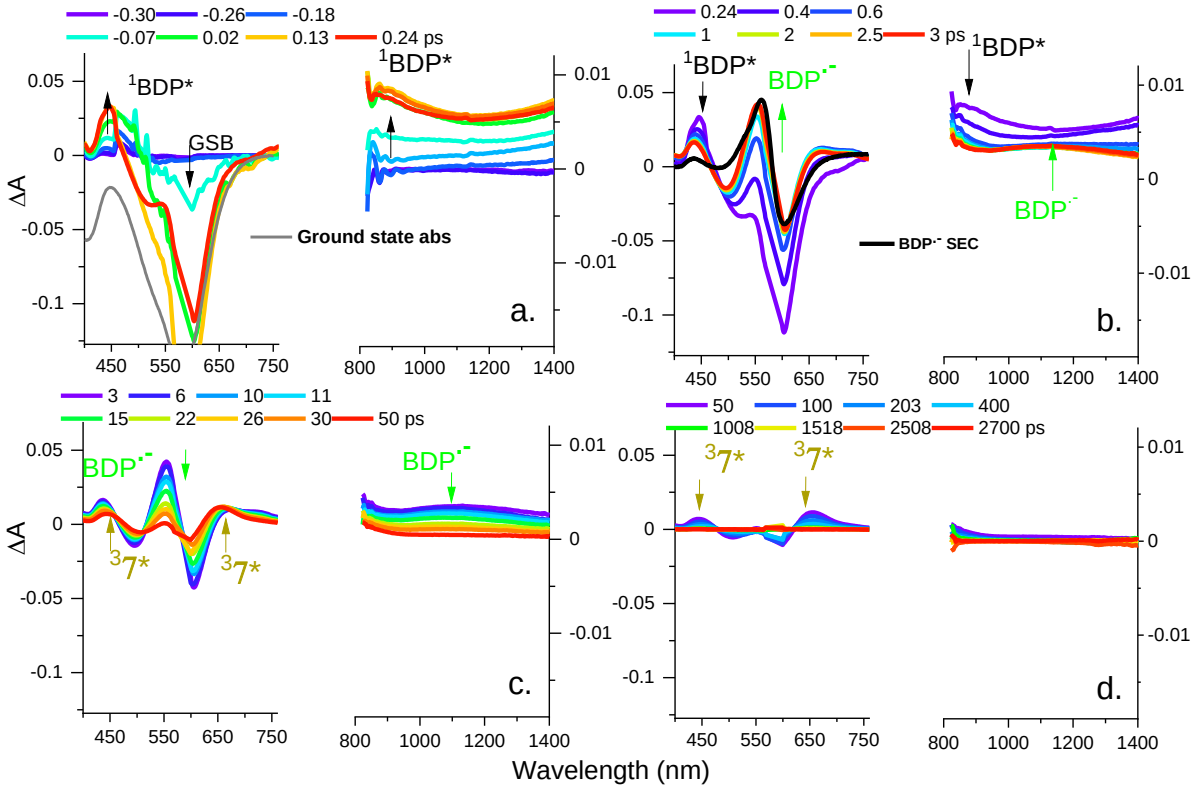

Figure 8. Femtosecond transient absorption spectra of [Fc]$_2$-BDP triad **7** (8 µM) at specified delay times: a − 0.3 to 0.24 ps; b 0.24 to 3 ps; c 3 to 100 ps and d 100 to 2700 ps in benzonitrile. λ_{exc} = 580 nm. The grey curve in panel (a) shows the inverted ground state absorption of **7** in benzonitrile and the black curve in panel (b) shows the spectroelectrochemical signature of one-electron reduced BDP unit in DCM.

Fitting of the TA kinetic traces (Figure 9) at specific probe wavelengths of 440, 555 and 673 nm corresponding to the overlapping TA signals of ^{1}BDP*, BDP$^{\cdot-}$, ^{3}BDP* converged with a multiexponential model, yielding 3 time constants of about 2 ps, 25 ps and 400 ps (Table 3). The 2 ps component is related to the decay of the excited BDP to undergo charge separation (Fc$^{\cdot+}$-BDP$^{\cdot-}$), which recombines in about 25 ps to populate the ^{3}**7***. The latter then decays to the ground state in about 400 ps. In the NIR region, the probe wavelength of 1150 nm is related to

the overlapping absorption of ^{1}BDP* and BDP$^{\cdot-}$, and the decay at this wavelength could be satisfactorily fit with two time-constants. The first time-constant of about 2 ps is attributed to the decay of ^{1}BDP* while the second of 25 ps corresponds to recombination of the charge-separated state (Fc$^{\cdot+}$-BDP$^{\cdot-}$).

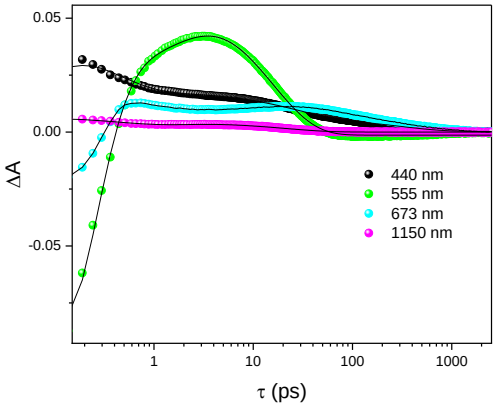

Figure 9. Multi-exponential fit of femtosecond transient absorption (λ_{exc} =580 nm) kinetic traces of the [Fc]$_2$-BDP triad **7** at specific wavelengths.

Table 3. Time constants obtained by multi-exponential fitting of kinetic traces of [Fc]$_2$-BDP triad **7** at specific wavelengths. *Benzonitrile solvent has strong contributions within 2 ps time windows.

Wavelength (nm)	**IRF* (ps)**	**A_1**	**τ_1 (ps)**	**A_2**	**τ_2 (ps)**	**A_3**	**τ_3 (ps)**
440 (^{1}BDP*, BDP$^{\cdot-}$ &^{3}BDP*)	0.7	0.03 (d)	2.0 ± 0.7 (^{1}BDP*)	0.01 (d)	26 ± 4 (BDP$^{\cdot-}$)	0.005 (d)	420 ± 18 (^{3}BDP*)
555 (GSB & BDP$^{\cdot-}$)	0.6	-0.04 (r)	2.0 ± 0.6 (BDP$^{\cdot-}$)	0.06 (d)	25 ± 4 (BDP$^{\cdot-}$)	-0.2 (r)	380 ± 26 (GSB)
673 (^{1}BDP* & ^{3}BDP*)	0.3	0.01 (d)	1.0 ± 0.5 (^{1}BDP*)	-0.005 (r)	26 ± 2 (^{3}BDP*)	0.005 (d)	370 ± 7 (^{3}BDP*)
1150 nm (^{1}BDP* & BDP$^{\cdot-}$)	0.3	0.001 (d)	2.0 ± 0.3 (^{1}BDP*)	0.001 (d)	25 ± 2 (BDP$^{\cdot-}$)		

ii. *Fc-BDP dyad **5***

Similarly, the femtosecond TA spectra and fitting of the kinetic traces for Fc-BDP dyad **5** are presented in Figures S53 and S54 and the fitting parameters are presented in Table S1 (see supporting information). The overlap of the kinetics of the Fc-BDP dyad **5** and [Fc]$_2$-BDP triad **7** at specific wavelengths corresponding to the ^{1}BDP* and BDP$^{\cdot-}$ radical anion, is presented in Figure S55 (supporting information). The TA kinetic traces of Fc-BDP dyad **5** exhibit very similar dynamic features as that of [Fc]$_2$-BDP triad **7**. It is worth noting that a very short lifetime

below the IRF was obtained in the TCSPC decay of Fc-BDP **5** (Figure 4 and Table 1), which can be related to the short component of about 3 ps obtained by femtosecond TA measurements.

These observations suggest that although the addition of two Fc units to the BDP moiety leads to a broader absorption of visible light due to extended conjugation and enhances the electronic coupling between Fc and BDP, it has no significant effect on the charge-separation and relaxation dynamics. The relaxation pathway of the Fc-BDP dyad **5** and $[Fc]_2$-BDP triad **7** is summarized in Figure 10.

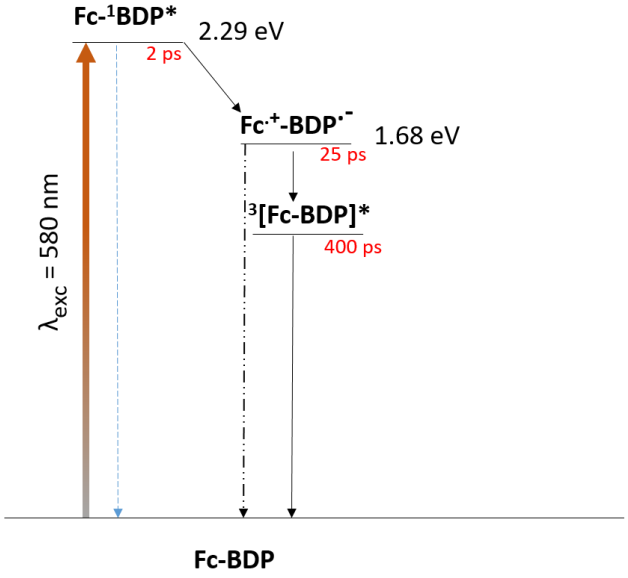

Figure 10. Energy level diagram presenting the photoinduced processes in the Fc-BDP dyad **5** and $[Fc]_2$-BDP triad **7** in argon-saturated benzonitrile. Energies: ^{1}BDP* of 2.29 eV is calculated from the mid-point of the absorption and emission spectra. The energy level of ^{3}[Fc-BDP]* lies between those of ^{3}BDP*[45] (1.55 eV) and ^{3}Fc*[35] (1.16 eV).

iii. *$[Fc]_2$-BDP-C_{60} tetrad **10***

Femtosecond transient absorption spectra of $[Fc]_2$-BDP-C_{60} tetrad **10** recorded in argon-saturated benzonitrile are shown in Figure 11. Similarly to the corresponding $[Fc]_2$-BDP triad **7**, the appearance of ^{1}BDP* bands were observed at 350 and 440 nm in the UV-visible region and broad absorption bands in the NIR, accompanied by a negative absorption band at about 550 nm. Additionally, a positive TA band appears at 1050 nm in the NIR region, which is associated with the C_{60} anion. The formation of the C_{60} anion was confirmed by overlapping the signature obtained by spectroelectrochemical (SEC) measurements (pink curve in panel (a) of Figure 11).[31] This is explained by an ultrafast electron transfer within the IRF from the Franck-Condon zone of ^{1}BDP* to C_{60}, forming Fc-BDP$^{\cdot+}$-$C_{60}^{\cdot-}$ in a folded conformer (Conformer 1) with a short center-to-center distance between BDP and C_{60}, which is in line with the ultrafast photoinduced electron transfer process observed in a similar BDP-C_{60} dyad.[33]

From 0.2 to 3 ps (Figure 11 in panel b), the ^{1}BDP* bands in the visible as well as NIR regions decay in the same time as the appearance of a new positive TA band at 550 nm attributed to the BDP$^{\cdot-}$ radical anion. This spectral feature can be attributed to an electron transfer step from Fc to ^{1}BDP* leading to a Fc$^{\cdot+}$-BDP$^{\cdot-}$-C_{60} ion pair in another conformer (Conformer 2) with a shorter center-to-center distance between Fc and BDP as compared to that of BDP and C_{60}. The

formation of $Fc^{\cdot+}$-$BDP^{\cdot-}$-C_{60} is consistent with the observations for the corresponding $[Fc]_2$-BDP triad **7** in the same time range (see Figure 8). Furthermore, a rapid electron transfer in the folded conformer (Conformer 1) from Fc to $BDP^{\cdot+}$ in the Fc-$BDP^{\cdot+}$-$C_{60}^{\cdot-}$ ion pair can take place in this time frame, resulting in the formation of a spatially distanced cation and anion radical pair ($Fc^{\cdot+}$-BDP-$C_{60}^{\cdot-}$). However, the transient species cannot be detected due to the low absorption of $Fc^{\cdot+}$.

In the third time window from 2 to 100 ps (panel c), the radical ion pair $Fc^{\cdot+}$-$BDP^{\cdot-}$-C_{60} of Conformer 2 recombines to populate the triplet excited state ^{3}[Fc-BDP]*-C_{60} localized on the BDP-Fc moiety, similarly to the corresponding triad **7** (Figure 8). No signature of $^3C_{60}$ was observed at longer delay times and in nanosecond transient absorption measurements,[28] excluding the population of this state after the charge recombination. In addition, the NIR part of this time window shows the decay of the transient bands corresponding to two processes: (i) decay of $Fc^{\cdot+}$-$BDP^{\cdot-}$-C_{60} of Conformer 2, consistent with the decay of $Fc^{\cdot+}$-$BDP^{\cdot-}$ in the $[Fc]_2$-BDP triad **7**, (See Figure 8) and (ii) decay of $Fc^{\cdot+}$-BDP-$C_{60}^{\cdot-}$ ion pair of Conformer 1. However the decay of $Fc^{\cdot+}$-BDP-$C_{60}^{\cdot-}$ is not complete and continues in the last time panel (d), beyond 100 ps. Finally, the decay of the triplet excited state ^{3}[Fc-BDP]*-C_{60} in the visible range is also observed in this last time window as already described for the $[Fc]_2$-BDP triad **7**.

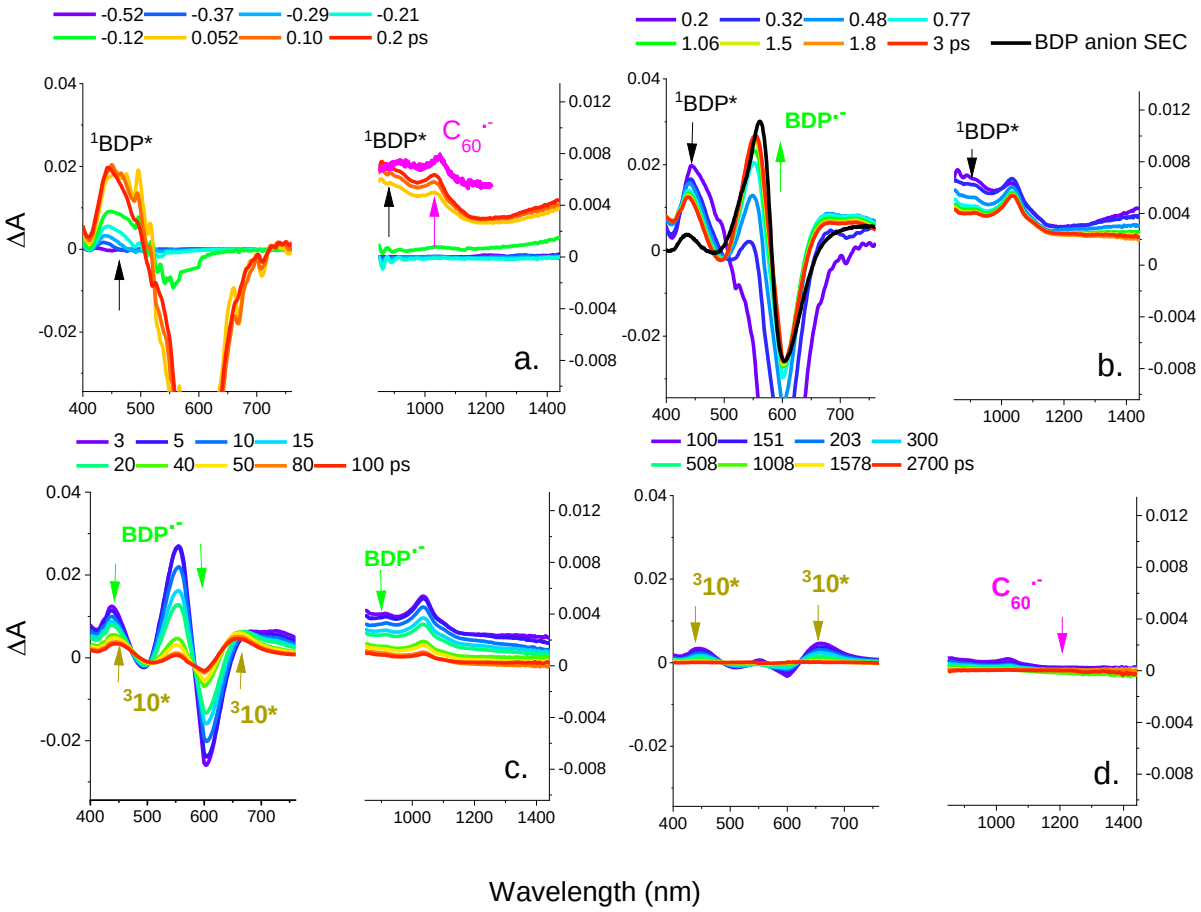

Figure 11. Femtosecond transient absorption spectra of $[Fc]_2$-BDP-C_{60} tetrad **10** (8 µM) at specified delay times: (a) − 0.5 to 0.2 ps; (b) 0.2 to 3 ps; (c) 3 to 100 ps and (d) 100 to 2700 ps in deaerated benzonitrile. λ_{exc} = 580 nm. The pink curve in panel (a) represents the SEC signature of C_{60} anion in DCM.

The fitting of kinetic traces at different probe wavelengths converged with a three exponential function yielding the time constants of about 3 ps, 25 ps and 400 ps (Figure 12 and Table 4). It is worth noting that the fitting did not yield the short component corresponding to the rise of $C_{60}^{\cdot-}$ occurring within the IRF. The 3 ps time-constant is attributed to the charge transfer from Fc to ^{1}BDP* to form Fc$^{\cdot+}$-BDP$^{\cdot-}$-C_{60}, (appearance of BDP$^{\cdot-}$ at 550 nm), which further recombines to populate ^{3}[Fc-BDP]*-C_{60} in about 25 ps (decay of BDP$^{\cdot-}$ at 550 and appearance of ^{3}[Fc-BDP]* at 673 nm). These time constants are in close agreement with those of isolated Fc-BDP dyad **5** and $[Fc]_2$-BDP triad **7**. The three-exponential fit of the 1050 nm kinetic trace also give three similar time-constants, but the longest time-constant of about 420 ps, which was not observed in the case of Fc-BDP **5** and **7** conjugates, is attributed to the decay of Fc$^{\cdot+}$-BDP-$C_{60}^{\cdot-}$ forming in Conformer 1.

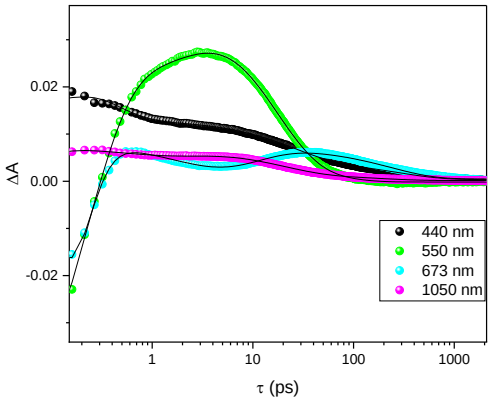

Figure 12. Multi-exponential fit of femtosecond transient absorption (λexc =580 nm) kinetic traces of the $[Fc]_2$-BDP-C_{60} tetrad **10** at specific wavelengths.

Table 4. Time constants obtained by multi-exponential fitting of kinetic traces of $[Fc]_2$-BDP-C_{60} tetrad **10** at specific wavelengths. *Benzonitrile solvent has strong contributions within the 2 ps time windows.

Wavelength (nm)	IRF* (ps)	A_1	τ_1 (ps)	A_2	τ_2 (ps)	A_3	τ_3 (ps)
440 (^{1}BDP*, ^{3}BDP* & BDP$^{\cdot-}$)	0.6	0.01 (d)	2.0 ± 0.6 (^{1}BDP*)	0.01 (d)	28 ± 7 (Fc$^{\cdot+}$+BDP$^{\cdot-}$-C_{60})	0.01 (d)	353 ± 60 (^{3}BDP*)
550 (GSB & BDP$^{\cdot-}$)	0.4	-0.02 (r)	3.0 ± 0.4 (Fc$^{\cdot+}$+BDP$^{\cdot-}$-C_{60})	0.03 (d)	27 ± 2 (Fc$^{\cdot+}$+BDP$^{\cdot-}$-C_{60})	-0.002	455 ± 4 (GSB)
673 (^{1}BDP* & ^{3}BDP*)	0.4	0.01 (d)	3.0 ± 0.5 (^{1}BDP*)	- 0.01 (r)	20 ± 1 (^{3}BDP*)	0.01 (d)	335 ± 9 (^{3}BDP*)
1050 (BDP$^{\cdot-}$ & $C_{60}^{\cdot-}$)	0.2	-0.01 (r)	2.0 ± 0.3 (Fc$^{\cdot+}$+BDP$^{\cdot-}$-C_{60})	0.01 (d)	23 ± 2 ps (Fc$^{\cdot+}$+BDP$^{\cdot-}$-C_{60})	0.001 (d)	420 ± 15 (Fc$^{\cdot+}$+BDP-$C_{60}^{\cdot-}$)

iv. *[Fc]-BDP-C_{60} triad* ***9***

The dynamics of Fc-BDP-C_{60} triad **9** presented in Figures S56, S57 and S58 (see supporting information for details) shows the same behavior as that of the tetrad **10**. The relaxation pathways upon photoexcitation of Fc-BDP-C_{60} triad **9** and $[Fc]_2$-BDP-C_{60} tetrad **10** are summarized schematically in Figure 13. Briefly, the excitation of the BDP unit in both assemblies at 580 nm leads to competitive rapid electron transfers in two conformers with varying distances between BODIPY and C_{60} due to the flexible linker between the two units.[33] Conformer 1, with a relatively short BDP and C_{60} distance, undergoes ultrafast electron transfer (<1 ps) to form a charge-separated state Fc-BDP$^{\cdot+}$-$C_{60}^{\cdot-}$, which further rapidly forms a longer lived (~400 ps) Fc$^{\cdot+}$-BDP-$C_{60}^{\cdot-}$ ion-pair. It is important to note that the lifetime of the Fc$^{\cdot+}$-BDP-$C_{60}^{\cdot-}$ is much longer than that of Fc$^{\cdot+}$-BDP$^{\cdot-}$ (25 ps) and of BDP$^{\cdot+}$-$C_{60}^{\cdot-}$ (40 ps) recently reported.[33] These findings highlight the effect of the multistep electron transfer mechanism in the Donor-Photosensitizer-Acceptor system resulting in a distant positioning of counter ions and thus stabilizing the charge-separated state. On the other hand, in Conformer 2, with a longer distance between BDP and C_{60}, an electron transfer preferably occurs from Fc to BDP giving rise to Fc$^{\cdot+}$-BDP$^{\cdot-}$-C_{60}, which recombines in 25 ps to populate ^{3}[Fc-BDP]*-C_{60}. The latter decays to the ground state with a time constant of about 400 ps, in a similar way as Fc-BDP **5** and **7** conjugates.

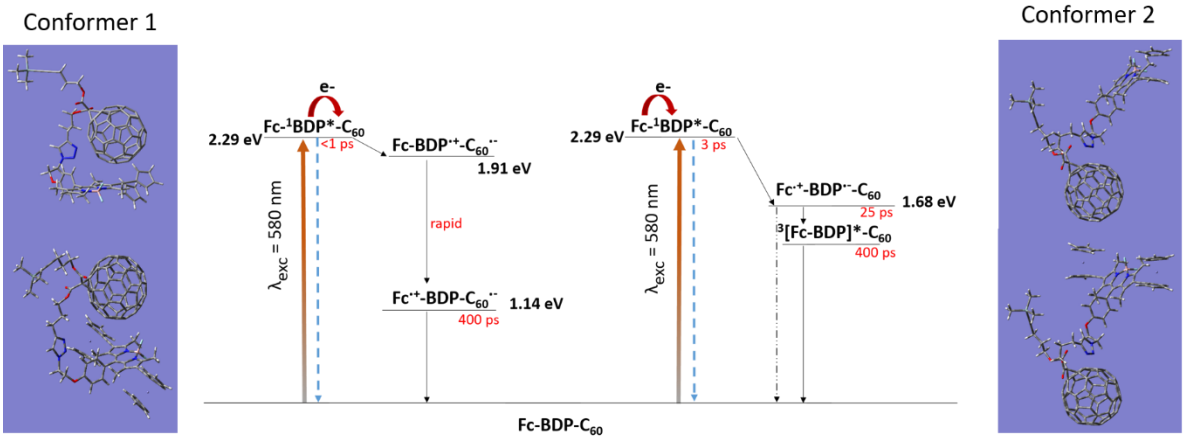

Figure 13. Energy level diagram presenting the photoinduced processes in the Fc-BDP-C_{60} triad **9** and $[Fc]_2$-BDP-C_{60} tetrad **10** in argon-saturated benzonitrile. Conformer 1 connotes a shorter BDP-C_{60} distance that undergoes ultrafast electron transfer from ^{1}BDP* to C_{60}. Conformer 2 with a shorter Fc and BDP distance compared to that of BDP and C_{60}, undergoes rapid electron transfer from Fc to ^{1}BDP*. Energies: ^{1}BDP* = 2.29 eV (calculated from the mid-point of the absorption and emission spectra of the Fc-BDP dyad **5**). The energy level of ^{3}[Fc-BDP]* lies between those of ^{3}BDP*[45] (1.55 eV) and ^{3}Fc*[35] (1.16 eV). On left : Conformer 1 of triad **9** and tetrad **10** obtained by semi-empirical calculations (PM6) ; On right : Conformer 2 of triad **9** and tetrad **10** obtained by semi-empirical calculations (PM6).

Conclusions

In summary, azido ferrocene-BODIPY conjugates in which one or two ferrocene entities are linked to the β-positions of the BODIPY core through an ethynyl bridge have been reported.

These derivatives were grafted under CuAAC conditions to a dual clickable fullerene platform bearing on one side an alkyne and on the other a protected alkyne. This post-functionalization approach allowed the high yield synthesis of new clickable Fc-BDP-C_{60} conjugates which have a reactive moiety available for further derivatisation. It is worth noting that while these assemblies could be prepared using classical fullerene chemistry (*ie* preforming ferrocene-BODIPY malonates followed by grafting to C_{60}) this method would have several drawbacks, including the formation of undesired poly-adducts with the loss of the complex ferrocene-BODIPY precursors, and recovery of the targets in low yields.

Photophysical investigations on the Fc-BDP-C_{60} triad and $[Fc]_2$-BDP-C_{60} tetrad along with the corresponding Fc-BDP and $[Fc]_2$-BDP conjugates were carried out by using steady-state and time-resolved absorption and emission spectroscopies. All conjugates display strong absorption in the visible region, which is bathochromically shifted when two ferrocenes are appended to the BODIPY core. In addition, the presence of one or two ferrocenes on the BODIPY broadens the absorption of these assemblies due to the extended conjugation and the overlapping charge transfer band from ferrocene to BODIPY. Femtosecond transient absorption studies revealed ultrafast multistep photoinduced electron transfers in the triad and tetrad leading to the formation of a spatially separated radical ion-pair ($Fc^{\bullet+}$-BDP-$C_{60}^{\bullet-}$). The latter exhibits a lifetime of about 400 ps which is the same order of magnitude as those of Fc-BDP-C_{60} conjugates previously reported.[34-35] It is also worth noting that the lifetime of $Fc^{\bullet+}$-BDP-$C_{60}^{\bullet-}$ is much longer than those in the corresponding dyads (BDP-C_{60} and Fc-BDP). Thus, the strategy of appending one or two additional donor units on the molecular dyad systems prolonged the lifetime of the charge-separated state.

Finally, the Fc-BDP-C_{60} conjugates developed in this work display the photophysical features required for solar energy conversion applications. Moreover, the presence of an available chemical functionality should allow the combination of these assemblies with complex structures such as inorganic compounds. This could contribute to the design of a new generation of multi-modular systems for artificial solar energy conversion.

Experimental Section

Materials and Methods

All organic reagents and solvents were purchased from commercial suppliers (Sigma-Aldrich, TCI, and others) and were used as received. Fullerene C_{60} (purity 99.5+%) was purchased from MTR Ltd. DCM was dried on $CaCl_2$ and distilled over CaH_2 prior to use. THF was distilled over sodium and benzophenone prior to use. Column chromatography was performed using silica gel 60 (0.040-0.063mm). Thin layer chromatography (TLC) was performed on aluminium sheets coated with silica gel 60 F_{254}. NMR spectra were performed in $CDCl_3$ at 25 °C on a Bruker Avance AM300 spectrometer. Chemical shifts were referenced to this internal solvent (7.26 for ^1H and 77.16 ppm for ^{13}C). Coupling constants (J values) are given in hertz (Hz). Splitting patterns are designated as s (singlet), bs (broad signal), d (doublet), t (triplet), q (quartet), and m (multiplet). High Resolution ESI-Mass spectra were recorded with a Waters Xevo Q-Tof instrument.

Methanofullerene platform 8 was prepared according to our previously reported procedure.[32] Parent BDP **1** has already been described in the literature and its synthesis and characterization is given in the supporting information.[46]

Steady-state absorption and fluorescence spectroscopy. A UV-2600 Shimadzu spectrophotometer was used to measure the ground state absorption spectra in the UV-visible range. With the help of Scientific Fluoromax PLUS, emission spectra were measured (Horiba Jobin-Yvon). The spectra were measured in quartz cells with an optical path of 1 cm, and the concentrations of the samples used for absorption and emission studies were in the micro-molar range.

Spectroelectrochemistry. A PalmSens4 potentiostat and an optically transparent thin layer electrochemical cell (OTTLE) were used to accomplish the spectroelectrochemical experiments. The cell uses a silver wire as a quasi-reference electrode, a platinum mesh as a working electrode, and a platinum wire as a counter electrode. Tetrabutylammonium hexafluorophosphate ($TBAPF_6$, 0.1 M) was used as a supporting electrolyte in dichloromethane. The spectra were measured in a Varian 5000 Cary spectrophotometer. Compounds of concentration of 10 µM in dichloromethane was used.

Time-correlated single-photon counting. Time-resolved fluorescence measurements were performed using the set-up previously described in the literature. [47] The BODIPY moieties in the Fc-BDP dyad **5** and the Fc-BDP-C_{60} triad **9** were excited at 495 nm. Using a Ti:sapphire laser (Coherent Chameleon Ultra II, 80 MHz) coupled to a pulse picker (4 MHz) and a harmonic generator (SHG/THG, APE), 495 nm femtosecond excitation pulses (<200 fs, FWHM, 4 MHz) were employed to excite the samples. Fluorescence emission was recorded at 555 nm, corresponding to the emission of BDP, using a FluoTime 200 spectrometer (4-nm bandpass) with polarizers at a magic angle. Fluorescence decays were then collected until a maximum of 10000 counts using a PicoHarp 300 TCSPC system (bin time = 4ps). The analyses of emission decay data were done with a weighted sum of exponential decays convolved by the IRF signal measured in a light-scattering Ludox colloidal solution, using the FluoFit software (PicoQuant). The full width at half maximum (FWHM) of IRF at 495 nm is 40 ps, which can be considered as the time-resolution of the measurements. Solutions with an absorbance below 0.1 (1 cm path-length) at excitation wavelengths were used. The quality of the fits was assessed by the value of χ^2 (<1.1), the weighted residuals and their autocorrelation function.

Femtosecond transient absorption. A commercial setup (Ultrafast Systems, Helios) was used to record femtosecond UV-Vis-NIR spectra.[48] The fundamental 800 nm beam was split into two beams to generate (a) a pump (λ_{exc} = 580 nm) in the optical parametric amplifier and (b) probe pulses, a white light continuum in the UV-Vis-NIR range (300 to 1400 nm) using either a CaF_2 plate (330-660 nm) or a sapphire plate (440-780 nm) or a YAG crystal (830-1400 nm). The pump energy was 2 µJ per pulse (beam size of 250 µm FWHM). The spectra were recorded in a 2 mm path length quartz cell under continuous stirring using a Teflon-coated bar. All measurements were performed in argon saturated solutions at room temperature. All the samples were scanned bi-directionally to ensure data reproducibility. The transient absorption data were corrected for the chirp of the white-light continuum using the Surface Xplorer program, supplied by the Ultrafast systems. The instrument response function (IRF) was around

200 fs (FWHM) but due to the strong benzonitrile solvent contribution within 2 ps time windows, a precise assignment of the shortest lifetime close to 1 ps could not be ascertained.

Synthetic Procedures

Synthesis of **compound 2.** To a 50 mL flask was added **compound 1** (100 mg, 0.25 mmol) in anhydrous DCM (15 mL). A solution of N-iodosuccinimide (64 mg, 0.28 mmol) in 5 mL DMF was added drop wise at 0°C. The mixture was stirred overnight at room temperature. The solvent mixture was evaporated. After purification by column chromatography on silica gel ($CHCl_3$/Et_2O 5%), an orange solid was obtained (90 mg, 66%). ^{1}H NMR (300 MHz, $CDCl_3$): δ 1.43 (s, 6H; -CH_3), 2.14 (bs, 1H; -OH), 2.55 (s, 3H, -CH_3), 2.62 (s, 3H, -CH_3), 4.03 (bs, 2H; -$\underline{CH_2}$-OH), 4.15 (t, *J* = 6.4 Hz, 2H; -CH_2-O-), 6.04 (s, 1H; -CH), 7.04 (d, *J* = 8.6 Hz, 2H, H_{arom}), 7.16 (d, *J* = 8.6 Hz, 2H; H_{arom}); ^{13}C NMR (75 MHz, $CDCl_3$): δ ^{13}C NMR (75 MHz, $CDCl_3$) δ 14.9 (-CH_3), 15.9 (-CH_3), 16.9 (-CH_3), 61.5 (-CH_2-OH), 69.3 (-CH_2-O-), 84.3 (C-I), 115.3 ($C_{BDP\text{-}arom}$), 122.3 (-CH), 127.4 , 129.27 , 131.4, 132.3, 141.5, 143.3, 145.2, 154.5, 157.8, 159.5 ($C_{BDP\text{-}arom}$); ^{19}F NMR (282 MHz, $CDCl_3$): δ -145.90 (q, *J* = 34.4 Hz); ^{11}B NMR (96 MHz, $CDCl_3$): δ 2.21 (t, *J* = 34.5 Hz); HRMS (ESI+): m/z calcd for $C_{21}H_{22}BF_2IN_2O_2Na$: 533.0685 $[M + Na]^+$, found: 533.0685.

Synthesis of **compound 3.** To a 50 mL flask was added **compound 1** (70 mg, 0.18 mmol) in anhydrous DCM (12 mL), then N-iodosuccinimide (165 mg, 0.73 mmol) was added. The mixture was stirred for 12 hours at room temperature under argon. The DCM was removed under reduced pressure. After purification by column chromatography on silica gel (DCM/Et_2O 95:5), a red solid was obtained (102 mg, 90%). ^{1}H NMR (300 MHz, $CDCl_3$): δ 1.44 (s, 6H; -CH_3), 2.05 (t, *J* = 6.02 Hz, 1H; -OH), 2.64 (s, 6H; -CH_3), 4.02-4.06 (m, 2H; -CH_2-OH), 4.17 (t, *J* = 6.4 Hz, 2H; -CH_2-O-), 7.06 (d, *J* = 8.6 Hz, 2H; H_{arom}), 7.15 (d, *J* = 8.6 Hz, 2H; H_{arom}); ^{13}C NMR (75 MHz, $CDCl_3$): δ 16.2 (-CH_3), 17.3 (-CH_3), 61.5 (-CH_2-OH), 69.4 (-CH_2-O-), 85.8 (C-I), 115.5 , 127.3, 129.3 , 131.8, 141.8, 145.4, 156.7, 159.7 (C_{BDP}-$_{arom}$); ^{19}F NMR (282 MHz, $CDCl_3$): δ -146.11 (q, *J* = 34.4 Hz); ^{11}B NMR (96 MHz, $CDCl_3$): δ 2.21 (t, *J*= 34.5 Hz); HRMS (ESI+): m/z calcd for $C_{21}H_{21}BF_2I_2N_2O_2Na$: 658.9651 $[M + Na]^+$, found: 658.9663.

Synthesis of **compound 4**. To a 25 mL flask under argon was added CuI (6 mg, 0.031 mmol), $Pd(PPh_3)_4$ (18 mg, 0.016 mmol), and **compound 2** (80 mg, 0.156 mmol) in THF (7 mL). Argon was bubbled through the solution for 30 min. Ethynylferrocene (131 mg, 0.63 mmol) and triethylamine (2 mL) were added. The mixture was heated overnight at 60°C under argon. The mixture was cooled to room temperature and concentrated under reduced pressure. After purification by column chromatography on silica gel (DCM/Et_2O 5%), a mauve solid was obtained (75 mg, 80%). ^{1}H NMR (300 MHz, $CDCl_3$): δ 1.45 (s, 3H; -CH_3), 1.51 (s, 3H; -CH_3), 2.03 (bs, 1H; -CH_2-$\underline{OH}$), 2.58 (s, 3H; -CH_3), 2.68 (s, 3H; -CH_3), 4.03 (bs, 2H; -$\underline{CH_2}$-OH), 4.16 (bs, 2H; -O-$\underline{CH_2}$-CH_2) 4.22-4.52 (m, 7H; H_{Fc}), 4.63 (bs, 2H; H_{Fc}), 6.01 (s, 1H; -CH), 7.05 (d, *J* = 7.9 Hz, 2H; H_{arom}), 7.18 (d, *J* = 7.9 Hz, 2H, H_{arom}); ^{13}C NMR (75 MHz, $CDCl_3$): δ 13.6, 13.7 (-CH_3), 14.8, 14.9 (-CH_3), 61.6 (-CH_2-OH), 69.4 (O-CH_2), 72.1 (C_{Fc}), 72.4 (C_{Fc}), 78.3, 94.6, 115.3 (CH_{arom}), 115.9, 122.0 (-CH_{BDP}), 127.4, 129.4 (CH_{arom}), 131.0, 132.9, 141.7, 142.6, 144.3, 156.9, 157.2, 159.4 (C_{BDP}-arom); ^{19}F NMR (282 MHz, $CDCl_3$): δ -146.33 (q, *J* = 32.3 Hz); ^{11}B

NMR (96 MHz, $CDCl_3$): δ 0.92 (t, *J* = 32.6 Hz). HRMS (ESI+): m/z calcd $C_{33}H_{31}BF_2FeN_2O_2$: 592.1796 [$M^{+\bullet}$], Found 592.1797.

Synthesis of **compound 5**. To a 25 mL flask under argon was added triphenylphosphine (PPh_3) (106 mg, 0.4 mmol), N-bromosuccinimide (NBS) (71 mg, 0.4 mmol), and **compound 4** (100 mg, 0.165 mmol) in dry 1,2-dichloroethane DCE (6 mL) at 0°C. The mixture was stirred at 0°C under argon until complete consumption of the starting material. Then 2 mL of a solution of sodium azide (25% aq) and 2 drops of Aliquat 336 were added, and the mixture was stirred overnight at 85 °C. The cooled mixture was washed with 20 mL of water, and the aqueous phase extracted with DCM. The combined organic phases were dried with $MgSO_4$, filtered and concentrated under reduced pressure. After purification by column chromatography on silica gel (DCM/Pentane 3/1), a mauve solid was obtained (50 mg, 50%). ^{1}H NMR (300 MHz, $CDCl_3$): δ 1.45 (s, 3H; -CH_3), 1.54 (s, 3H; -CH_3), 2.57 (s, 3H; -CH_3), 2.68 (s, 3H, -CH_3), 3.66 (t, *J* =4.8 Hz, 2H; -CH_2-N_3), 4.14-4.27 (m, 9H; H_{Fc}, -CH_2-O-), 4.42-4.48 (m, 2H; H_{Fc}), 6.02 (s, 1H; -CH), 7.05 (d, *J* = 8.5 Hz, 2H; H_{arom}), 7.19 (d, *J* = 8.5 Hz, 2H; H_{arom}); ^{13}C NMR (75 MHz, $CDCl_3$): δ 13.6, 13.7 (-CH_3), 14.8, 14.9 (-CH_3), 50.3 (-CH_2-N_3), 65.6 (C_{Fc}), 67.1 (-CH_2-O-), 68.9, 70.1, 70.2, 71.5 (C_{Fc}), 94.6 (C_{alkyne}), 115.3 ($C_{BDP\text{-}arom}$), 116.2 (C_{alkyne}), 121.9 (-CH), 127.6, 129.4, 130.8, 132.8, 141.8, 142.6, 143.3, 156.7, 157.1, 159.0 ($C_{BDP\text{-}arom}$); ^{19}F NMR (282 MHz, $CDCl_3$): δ -146.27 (q, *J* = 32.1 Hz); ^{11}B NMR (96 MHz, $CDCl_3$): δ 0.71 (t, *J* = 34.3 Hz); HRMS (ESI+): m/z calcd for $C_{33}H_{30}BF_2FeN_5O$: 617.1861 [$M^{+\bullet}$]; found: 617.1865.

Synthesis of **compound 6.** To a 25 mL flask under argon was added CuI (15 mg, 0.078 mmol), $Pd(PPh_3)_4$ (44 mg, 0.038 mmol), and **compound 3** (80 mg, 0.126 mmol) in THF (10 mL). Argon was bubbled through the solution for 30 min. Ethynylferrocene (108 mg, 0.51 mmol) and triethylamine (4 mL) were added. The mixture was heated overnight at 60°C under argon. The mixture was cooled to room temperature and concentrated under reduced pressure. After purification by column chromatography on silica gel (DCM/Et_2O 5%), a mauve solid was obtained (77 mg, 76%). ^{1}H RMN (300 MHz, $CDCl_3$): δ 1.56 (s, 6H; -CH_3), 2.07 (bs, 1H; -OH), 2.69 (s, 6H; -CH_3),4.04 (bs, 2H; -$\underline{CH_2}$-OH), 4.16 – 4.22 (m, 16H; H_{Fc} et -CH_2-O-), 4.45 (m, 4H; H_{Fc}), 7.07 (d, *J* = 8.5 Hz, 2H; H_{arom}), 7.20 (d, *J* = 8.4 Hz, 2H; H_{arom}); ^{13}C NMR (75 MHz, $CDCl_3$): δ 13.8 (CH_3), 61.5 (-CH_2-OH), 65.5, 69.0 (C_{Fc}), 69.4 (-CH_2-O), 70.1, 71.6 (C_{Fc}), 95.2 (C_{alkyne}), 115.4, 116.9, 127.2, 129.4, 131.7, 142.1, 143.5, 158.1, 159.6 ($C_{BDP\text{-}arom}$); ^{19}F NMR (282 MHz, $CDCl_3$): δ -146.38 (q, *J* = 32 Hz); ^{11}B NMR (96 MHz, $CDCl_3$): δ 2.08 (t, *J* = 32.0 Hz). HRMS (ESI+): m/z calcd for $C_{45}H_{39}BF_2Fe_2N_2O_2$: 800.1771 [$M^{+\bullet}$], found 800.1783.

Synthesis of **compound 7.** To a 25 mL flask under argon was added PPh_3 (133 mg, 0.5 mmol), NBS (90 mg, 0.5 mmol), and **compound 6** (185 mg, 0.23 mmol) in dry DCE (10 mL) at 0°C. The mixture was stirred at 0°C under argon until complete consumption of the starting material. Then 3 mL of a solution of NaN_3 (25% aq) and 2 drops of Aliquat 336 were added, and the mixture was stirred overnight at 85 °C. The cooled mixture was washed with 20 mL of water, and the aqueous phase extracted with DCM. The combined organic phases were dried with $MgSO_4$, filtered and concentrated under reduced pressure. After purification by column chromatography on silica gel (DCM/Pentane 8/3), a mauve solid was obtained (90 mg, 47%). ^{1}H NMR (300 MHz, $CDCl_3$): δ 1.56 (s, 6H; -CH_3), 2.70 (s, 6H; -CH_3), 3.67 (t, *J* = 4.4 Hz, 2H; -CH_2-N_3), 4.15-4.28 (m, 16H; H_{Fc} and -CH_2-O-), 4.41-4.52 (m, 4H; H_{Fc}), 7.07 (d, *J* = 8.4 Hz,

2H; H_E or H_F), 7.21 (d, *J* = 8.4 Hz, 2H; H_E or H_F); ^{13}C NMR (75 MHz, $CDCl_3$): δ 13.8 (-CH_3), 50.4 (-CH_2-N_3), 65.5 (-CH_2-O-), 67.1, 69.0, 70.1, 71.7 (C_{Fc}), 95.2 (C_{alkyne}), 115.4, 116.9, 127.5, 129.5, 131.6, 141.9, 143.5, 158.1, 159.1 ($C_{BDP\text{-}arom}$); ^{19}F NMR (282 MHz, $CDCl_3$): δ -146.39 (q, *J* = 32.1 Hz); ^{11}B NMR (96 MHz, $CDCl_3$): δ 0.63 (t, *J* = 34.3 Hz); HRMS (ESI+): m/z calcd for $C_{45}H_{38}BF_2Fe_2N_5O$: 825.1836 [$M^{+\bullet}$] ; found: 825.1844.

Synthesis of **Compound 9**. To a 25 mL flask under argon was added **compound 8** (125 mg, 0.122 mmol) in dry DCM (15 mL). Argon was bubbled through the solution for 30 minutes, then **compound 5** (60mg, 0.096 mmol), DIPEA (16 μL, 0.096 mmol), and CuBr (14 mg, 0.096 mmol) were added. The mixture was stirred overnight at room temperature under argon. The solution was washed with an aqueous solution of EDTA (40 ml, 0.05 M), then 20 mL of water. and the aqueous phases were extracted with DCM. The combined organic phases were dried with $MgSO_4$, filtered, and concentrated under reduced pressure. After purification by column chromatography on silica gel ($CHCl_3$/Et_2O 100/7), a mauve solid was obtained (145 mg, 91%). ^{1}H NMR (300 MHz, $CDCl_3$): δ 0.16 (s, 9H; H_n), 1.42 (s, 3H; H_D), 1.49 (s, 3H; H_D), 1.95-2.16 (m, 2H; H_j), 2.24-2.30 (m, 2H; H_d), 2.43 (t, *J* = 6.9 Hz, 2H; H_k), 2.55 (s, 3H, H_A), 2.66 (s, 3H; H_A), 2.96 (t, *J*= 7.1 Hz, 2H; Hc), 4.18-4.21 (m, 7H; H_{Fc}), 4.39-4.48 (m, 4H; H_H, H_{Fc}), 4.51-4.65 (m, 4H; H_e, H_i), 4.73-4.84 (m, 2H; H_G), 6.00 (s, 1H; H_B), 7.01 (d, *J* = 8.5 Hz, 2H; H_E or H_F), 7.17 (d, *J* = 8.5 Hz, 2H; H_E or H_F), 7.61 (s, 1H, H_a); ^{13}C NMR (75 MHz, $CDCl_3$): δ 0.29 (C_n), 13.5 (C_D), 14.8 (C_A), 15.0 (C_A), 16.7 (C_k), 22.1 (H_c), 27.7, 28.2 (C_d, C_j), 49.5 (C_H), 52.1 (C_g), 65.6, 66.0 (C_e, C_i), 66.5 (C_G), 66.6, 68.9, 70.1, 71.7 (C_{Fc}), 86.2 (C_m), 94.7 ($C_{alkyne\text{-}BDP}$), 105.2 (C_l), 115.4 ($C_{BDP\text{-}arom}$), 122.05 (C_B), 122.6 (C_a), 128.1, 129.6, 132.6 ($C_{arom\text{-}BDP}$), 139.1, 139.2, 141.1, 141.2, 141.5, 141.9, 142.0, 142.3, 142.5, 143.1, 143.2, 143.3, 144.0, 144.7, 144.81, 144.84, 145.1, 145.2, 145.3, 145,36, 145.41, 145.44, 145.6, 145.6 ($C_{BDP\text{-}arom}$ and C_{60}, C_{sp2}), 156.8, 157.2, 158.6 ($C_{BDP\text{-}arom}$), 163.7 (C_f, C_h); ^{19}F NMR (282 MHz, $CDCl_3$): δ -146.24 (q, *J* = 34.4 Hz); ^{11}B NMR (96 MHz, $CDCl_3$): δ 0.67 (t, *J*= 34.5 Hz); HRMS (ESI+): calcd for $C_{109}H_{52}BN_5O_5F_2SiFe$: 1642.3185 [$M^{+\bullet}$]; found: 1642.3168.

Synthesis of **compound 10.** To a 25 mL flask under argon was added **compound 8** (85 mg, 0.082 mmol) in dry DCM (15 mL). Argon was bubbled through the solution for 30 minutes, then **compound 7** (50 mg, 0.06 mmol), DIPEA (10 μL, 0.06 mmol), and CuBr (9 mg, 0.06 mmol) were added. The mixture was stirred overnight at room temperature under argon. The solution was washed with an aqueous solution of EDTA (40 ml, 0.05 M), then 20 mL of water. and the aqueous phases were extracted with DCM. The combined organic phases were dried with $MgSO_4$, filtered, and concentrated under reduced pressure. After purification by column chromatography on silica gel (DCM/Et_2O 100/6), a mauve solid was obtained (85 mg, 77%). ^{1}H NMR (300 MHz, $CDCl_3$): δ: 0.16 (s, 9H; H_n), 1.51 (s, 6H; C_A), 1.95-2.19 (m, 2H; H_j), 2.20-2.30 (m, 2H; H_d), 2.43 (t, *J* = 6.9 Hz, 2H; H_k), 2.67 (s, 6H; H_D) 2.96 (t, *J* = 7.2 Hz, 2H; Hc,), 4.13-4.16 (m, 16H; H_{Fc}), 4.40.-4.47 (m, 6H; H_H, H_{Fc}), 4.50-4.64 (m, 4H; H_e, H_i), 4.75-4.84 (m, 2H; H_G), 7.04 (d, *J* = 8.5 Hz, 2H; H_E or H_F), 7.17 (d, *J* = 8.5 Hz, 2H; H_E or H_F), 7.63 (s, 1H; H_a); ^{13}C NMR (75 MHz, $CDCl_3$): 0.3 (C_n), 13.9 (C_D, C_A), 16.7 (C_k), 22.1 (H_c), 27.7, 28.2 (C_d, C_j), 49.7 (C_H), 52.3 (C_g), 65.6, 66.1 (C_e, C_i), 66.7 (C_G), 69.0, 70.1, 71.6 (C_{Fc}), 86.2 (C_m), 95.3 ($C_{alkyne\text{-}BDP}$), 105.2 (C_l), 115.5 ($C_{arom\text{-}BDP}$), 122.7 (C_a), 128.1 ($C_{arom\text{-}BDP}$), 129.6, 131.5 ($C_{arom\text{-}BDP}$), 139.1, 139.2, 141.1, 141.2, 141.6, 141.64, 141.9, 142.0, 142.3, 143.1, 143.2, 143.3, 144.1, 144.7, 144.81, 144.84, 145.1, 145.2, 145.3, 145,4, 145.41, 145.43, ($C_{arom\text{-}BDP}$ and C_{60}, C_{sp2}),

158.2, 158.7 ($C_{arom\text{-}BDP}$), 163.7 (C_f, C_h); ^{19}F NMR (282 MHz, $CDCl_3$): δ: -145.31 (q, *J* = 34.4 Hz); ^{11}B NMR (96 MHz, $CDCl_3$): δ: 0.59 (t, *J* = 34.5 Hz); HRMS (ESI+): calcd for $C_{121}H_{61}BN_5O_5F_2SiFe_2$ $[M+H]^+$: 1851.3238, found: 1851.3208.

Supplementary Material

Supporting information for this article is available on the WWW under http://dx.doi.org/10.1002/MS-number.

Acknowledgements

This work was supported by the CNRS (International Emerging Action, PICS project no 08198), the LabEx PALM ANR-10LABX-0039-PALM and CHARMMMAT ANR-11-LABX-0039, Région Ile-de-France DIM NanoK, the University of Versailles St-Quentin-en-Yvelines and University of Paris-Saclay. Chevreul Institute (FR 2638), Ministère de l'Enseignement Supérieur, de la Recherche et de l'Innovation, Hauts-de-France Region and FEDER are acknowledged for supporting and funding partially this work giving access to fluorescence time resolved experiments. J. Rabah thanks the MESRI « Ministère de l'Enseignement Supérieur de la Recherche et de l'Innovation » for a PhD fellowship (2017-2020). A. Fatima is grateful for the MESRI grant (2019-2022).

Author contributions

J. Rabah, K. Wright and M. Gueye synthesized the compounds, performed their analysis by NMR spectroscopy. J. Rabah and A. Vallée performed their analysis by electrochemistry. J. Rabah and A. Fatima performed the absorption and fluorescence experiments, A. Fatima, M. Sliwa and G. Clavier performed time-resolved fluorescence measurements. G. Clavier performed the semi-empirical calculations. A. Fatima, J. Pham and F. Miomandre did spectroelectrochemical experiments, A. Fatima, G. Burdzinski and M.-H. Ha-Thi performed transient absorption measurements. A. Fatima, G. Burdzinski, M.-H. Ha-Thi, R. Méallet-Renault, K. Steenkeste and T. Pino made the data analysis and interpretation of transient absorption measurements. J. Rabah, A. Fatima, M.-H. Ha-Thi, K. Wright, H. Fensterbank and E. Allard wrote the original manuscript. All authors have read and agreed to the submitted version of the manuscript.

Entry for the Table of Contents

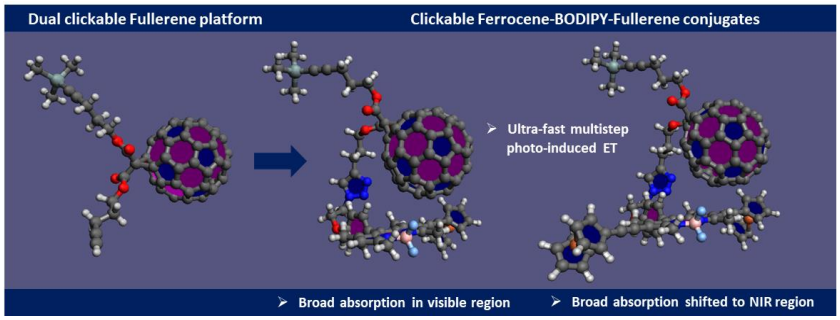

Twitter

Donor-acceptor conjugates containing Ferrocene-BODIPY-fullerene moieties were synthesized and characterized by photophysical methods for potential applications in solar energy conversion.
Institut Lavoisier Versailles
@ILV_UMR8180

References

[1] E. Nakamura, H. Isobe, 'Functionalized Fullerenes in Water. The First 10 years of Their Chemistry, Biology, and Nanoscience' *Acc. Chem. Res.* **2003**, *36*, 807-815.
[2] F. Cataldo, T. Da Ros, in 'Carbon Materials: Chemistry and Physics', Eds F. Cataldo, P. Milani, Springer: Dordrecht, 2008; Vol. 1.
[3] V. Biju, 'Chemical modifications and bioconjugate reactions of nanomaterials for sensing, imaging, drug delivery and therapy' *Chem. Soc. Rev.* **2014**, *43*, 744-764.
[4] J. L. Segura, N. Martín, D. M. Guldi, 'Materials for organic solar cells: the C60/π-conjugated oligomer approach', *Chem. Soc. Rev.* **2005**, *34*, 31-47.
[5] E. Espíldora, J. L. Delgado, N. Martín, 'Donor-Acceptor Hybrids for Organic Electronics', *Isr J. Chem.* **2014**, *54*, 429-439.
[6] M. A. Lebedeva, T. W. Chamberlain, A. N. Khlobystov, 'Harnessing the Synergistic and Complementary Properties of Fullerene and Transition-Metal Compounds for Nanomaterial Applications', *Chem. Rev.* **2015**, *115*, 11301-11351.
[7] O. Ito, 'Photosensitizing Electron Transfer Processes of Fullerenes, Carbon Nanotubes, and Carbon Nanohorns', *Chem. Rec.* **2017**, *17*, 326-362.
[8] A. Zieleniewska, F. Lodermeyer, A. Roth, D. M. Guldi, 'Fullerenes – how 25 years of charge transfer chemistry have shaped our understanding of (interfacial) interactions', *Chem. Soc. Rev.* **2018**, *47*, 702-714.
[9] A. Hirsch, M. Brettreich, in 'Fullerenes: Chemistry and Reactions', Wiley-VCH, Weinheim, **2005**.
[10] A. M. López, A. Mateo-Alonso, M. Prato, 'Materials chemistry of fullerene C_{60} derivatives', *J. Mater Chem.* **2011**, *21*, 1305-1318.
[11] Nierengarten, I.; Nierengarten, 'The Impact of Copper-Catalyzed Alkyne-Azide 1,3-dipolar Cycloaddition in Fullerene Chemistry', J.-F. *Chem. Rec.* **2015**, *15*, 31-51.
[12] H. Lu, J. Mack, Y. Yang, Z. Shen, 'Structural modification strategies for the rational design of red/NIR region BODIPYs', *Chem. Soc. Rev.* **2014**, *43*, 4778-4823.
[13] N. Boens, B. Verbelen, M. J. Ortiz, L. Jiao, W. Dehaen, 'Synthesis of BODIPY dyes through postfunctionalization of the boron dipyrromethene core', *Coord. Chem. Rev.* **2019**, *399*, 213024-213108.
[14] M. E. El-Khouly, S. Fukuzumi, F. D'Souza, 'Photosynthetic Antenna-Reaction Center Mimicry by Using Boron Dipyrromethene Sensitizers', *ChemPhysChem* **2014**, *15*, 30-47.
[15] C. O. Obondi, G. N. Lim, P. A. Karr, V. N. Nesterov, F. D'Souza, 'Photoinduced charge separation in wide-band capturing, multi-modular bis(donor styryl)BODIPY-fullerene systems', *Phys. Chem. Chem. Phys.* **2016**, *18*, 18187-18200.
[16] J.-Y. Liu, X.-N. Hou, Y. Tian, L. Jiang, S. Deng, B. Röder, E. A. Ermilov, 'Photoinduced energy and charge transfer in a bis(triphenylamine)-BODIPY-C_{60} artificial photosynthetic system', *RSC Adv.* **2016**, *6*, 57293-57305.
[17] S. Shao, H. B. Gobeze, P. A. Karr, F. D'Souza, ' "Two-Point" Self-Assembly and Photoinduced Electron Transfer in *meso*-Donor-Carrying Bis(styryl crown ether)-BODIPY-Bis(alkylammonium)fullerene Donor-Acceptor conjugates', *Chem. Asian. J.* **2017**, *12*, 2258-2270.
[18] D. Gao, S. M. Aly, P.-L. Karsenti, G. Brisard, P. D. Harvey, 'Ultrafast energy and electron transfers in structurally well addressable BODIPY-porphyrin-fullerene polyads', *Phys. Chem. Chem. Phys.* **2017**, *19*, 2926-2939.

[19] C. O. Obondi, G. N. Lim, P. Martinez, V. Swamy, F. D'Souza, 'Controlling electron and energy transfer paths by selective excitation in a zinc porphyrin-BODIPY-C_{60} multi-modular triad', *Nanoscale* **2017**, *9*, 18054-18065.
[20] N. Zarrabi, C. O. Obondi, G. N. Lim, S. Seetharaman, B. G. Boe, F. D'Souza, P. K. Poddutoori, 'Charge-separation in a panchromatic, vertically positioned bis(donor styryl)BODIPY-aluminum(III)porphyrin-fullerene supramolecular triads', *Nanoscale* **2018**, *10*, 20723-20739.
[21] S. Shao, M. B. Thomas, K. H. Park, Z. Mahaffey, D. Kim, F. D'Souza, 'Sequential energy transfer followed by electron transfer in a BODIPY-bisstyrylBODIPY bound to C_{60} triad via a 'two-point' binding strategy', *Chem. Commun*. **2018**, *54*, 54-57.
[22] A. Cabrera-Espinoza, B. Insuasty, A. Ortiz, 'Novel BODIPY-C_{60} derivatives with tuned photophysical and electron-acceptor properties : Isoxazolino[60]fullerene and pyrrolidino[60]fullerene', *J. Lumin.* **2018**, *194*, 729-738.
[23] K. Calderon-Cerquera, A. Parra, D. Madrid-Úsuga, A. Cabrera-Espinoza, C. A. Melo-Luna, J. H. Reina, B. Insuasty, A. Ortiz, 'Synthesis, characterization and photophysics of novel BODIPY linked to dumbbell systems based on Fullerene[60]pyrrolidine and Fullerene[60] isoxazoline', *Dyes and Pigments* **2021**, *184*, 108752-108760.
[24] P. Wang, W. Wu, J. Zhao, D. Huang, X. Yi, 'Using C_{60}-bodipy dyads that show strong absorption of visible light and long-lived triplet excited state as organic triplet photosensitizers for triplet-triplet annihilation upconversion', *J. Mater. Chem.* **2012**, *22*, 20273-20283.
[25] W. Wu, J. Zhao, J. Sun, S. Guo, 'Light-Harvesting Fullerene Dyads as Organic Triplet Photosensitizers for Triplet-Triplet Annihilation Upconversions', *J. Org. Chem.* **2012**, *77*, 5305-5312.
[26] S. Guo, L. Xu, K. Xu, J. Zhao, B. Küçükoz, A. Karatay, H. G. Yaglioglu, M. Hayvaldi, A. Elmali, 'Bodipy-C60 triple hydrogen bonding assemblies as heavy atom-free triplet photosensitizers: preparation and study of the singlet/triplet energy transfer', *Chem. Sci.* **2015**, *6*, 3724-3737.
[27] Y. Wei, M. Zhou, Q. Zhou, X. Zhou, S. Liu, S. Zhang, B. Zhang, 'Triplet-triplet annihilation upconversion kinetics of C_{60}-Bodipy dyads as organic triplet photosensitizers', *Phys. Chem. Chem. Phys.* **2017**, *19*, 22049-22060.
[28] A. Fatima, J. Rabah, E. Allard, H. Fensterbank, K. Wright, G. Burdzinski, G. Clavier, M. Sliwa, T. Pino, R. Méallet-Renault, K. Steenkeste, M.-H. Ha-Thi, 'Selective population of triplet excited states in heavy-atom-free BODIPY-C_{60} based molecular assemblies', *Photochem. Photobiol. Sci.* **2022**, *21*, 1573-1584.
[29] P De Bonfils, L. Péault, P. Nun, V. Coeffard, 'State of the Art of Bodipy-Based Photocatalyst in Organic Synthesis', *Eur. J. Org. Chem.* **2021**, 1809-1824.
[30] H. Fensterbank, K. Baczko, C. Constant, N. Idttalbe, F. Bourdreux, A. Vallée, A.-M. Goncalves, R. Méallet-Renault, G. Clavier, K. Wright, E. Allard, 'Sequential Copper-Catalyzed Alkyne-Azide Cycloaddition and Thiol-Maleimide Addition for the Synthesis of Photo- and/or Electroactive Fullerodendrimers and Cysteine-Functionalized Fullerene Derivatives', *J. Org. Chem*. **2016**, *81*, 8222-8233.
[31] T.-T. Tran, J. Rabah, M.-H. Ha-Thi, E. Allard, S. Nizinski, G. Burdzinski, S. Aloïse, H. Fensterbank, K. Baczko, H. Nasrallah, A. Vallée, G. Clavier, F. Miomandre, T. Pino, R. Méallet-Renault, 'Photoinduced Electron Transfer and Energy Transfer Processes in a Flexible BODIPY-C_{60} dyad', *J. Phys. Chem B* **2020**, *124*, 9396-9410.
[32] J. Rabah, L. Yonkeu, K. Wright, A. Vallée, R. Méallet-Renault, M.-H. Ha-Thi, A. Fatima, G. Clavier, H. Fensterbank, E. Allard, 'Synthesis of a dual clickable fullerene platform and construction of a dissymmetric BODIPY-[60]Fullerene-DistryrylBODIPY triad', *Tetrahedron* **2021**, *100*, 132467-132476.
[33] A. Fatima, J. Rabah, E. Allard, H. Fensterbank, K. Wright, G. Burdzinski, F. Miomandre, J. Pham, G. Clavier, M. Sliwa, T. Pino, R. Méallet-Renault, K. Steenkeste, M.-H. Ha-Thi, 'Ultrafast time-resolved spectroscopy elucidating photo-driven electron and energy transfer processes in a broadband light-absorbing BODIPY-C_{60}-distyryl BODIPY triad', *Eur. Phys. J. Spec. Top.* **2022**. *https://doi.org/10.1140/epjs/s11734-022-00670-y*
[34] C. A. Wijesinghe, M. E. El-Khouly, J. D. Blakemore, M. E. Zandler, S. Fukuzumi, F. D'Souza, 'Charge stabilisation in a closely spaced ferrocene-boron-dipyrrin-fullerene triad', *Chem. Commun.* **2010**, *46*, 3301-3303.

[35] J.-Y Liu, M. E. El-Khouly, S. Fukuzumi, D. K. P. Ng, 'Photoinduced Electron Transfer in a Ferrocene-Distyryl BODIPY Dyad and a Ferrocene Distyryl BODIPY-C_{60} Triad', *ChemPhysChem* **2012**, *13*, 2030-2036.
[36] Y. V. Zatsikha, R. K. Swedin, A. T. Healy, P. C. Goff, N. O . Didukh, T. S. Blesener, M. Kayser, Y. P. Kovtun, D. A. Blank, V. N. Nemykin, 'Synthesis, Characterization, and Electron-Transfer Properties of Ferrocene-BODIPY-Fullerene Near-Infrared-Absorbing Triads: Are Catecholopyrrolidine-Linked Fullerenes a Good Architecture to Facilitate Electron Transfer ?', *Chem. Eur. J.* **2019**, *25*, 1-15.
[37] B. Dhokale, P. Gautam, S. M. Mobin, R. Misra, 'Donor-Acceptor, ferrocenyl substituted BODIPYs with marvelous supramolecular interactions', *Dalton Trans.* **2013**, *42*, 1512–1518.
[38] P. Gautam, B. Dhokale, S. M. Mobin, R. Misra, 'Ferrocenyl BODIPYs: synthesis, structure and properties', *RSC Adv.* **2012**, *2*, 12105–12107.
[39] Y. Chen, J. Zhao, H. Guo, L. Xie, 'Geometry Relaxation-Induced Large Stokes Shift in Red-Emitting Borondipyrromethenes (BODIPY) and Applications in Fluorescent Thiol Probes', *J. Org. Chem.* **2012**, *77*, 2192-2206.
[40] X. Wu, W. Wu, X. Cui, J. Zhao, M. Wu, 'Preparation of Bodipy-ferrocene dyads and modulation of the singlet/triplet state excited state of bodipy via electron transfer and triplet energy transfer', *J. Mater. Chem. C* **2016**, *4*, 2843-2853.
[41] A. Loudet, K. Burgess, 'BODIPY Dyes and Their Derivatives: Syntheses and Spectroscopic Porperties', *Chem. Rev.* **2007**, *107*, 4891-4932.
[42] D. M. Guldi, H. Hungerbühler, I. Carmichael, K.-D. Asmus, M. Maggini, '[6-6]-Closed versus [6-5]-Open Isomers of Imino- and Methanofullerenes: A Comparison with Pristine C_{60} and $(C_{59}N)^{\bullet}$', *J. Phys. Chem. A* **2000**, *104*, 8601-8608.
[43] A. Paul, R. Borrelli, H. Bouyanfif, S. Gottis, F. Sauvage, 'Tunable Redox Potential, Optical Properties, and Enhanced Stability of Modified Ferrocene-Based Complexes', *ACS Omega* **2019**, *4*, 14780-14789.
[44] C.-L. Liu, Y. Chen, D. P. Shelar, C. Li, G. Cheng, W.-F. Fu, 'Bodipy dyes bearing oligo(ethylene glycol) groups on the meso-phenyl ring: tuneable solid-state photoluminescence and highly efficient OLEDs', *J. Mater. Chem. C* **2014**, *2*, 5471–5478.
[45] W. Wu, H. Guo, W. Wu, S. Ji, J. Zhao, 'Organic Triplet Sensitizer Library Derived from a Single Chromophore (BODIPY) with Long-Lived Triplet Excited State for Triplet-Triplet Annihilation Based Upconversion', *J. Org. Chem.* **2011**, *76*, 7056-7064.
[46] J. Shen, Q. Wang, Y. Lv, J. Dong, G. Xuan, J. Yang, D. Wu, J. Zhou, G. Yu, G. Tang, X. Li, F. Huang, X. Chen, 'Nanomedecine fabricated from a boron-dipyrromethene (BODIPY)-embedded amphiphilic copolymer for photothermal-enhanced chemotherapy', *ACS Biomater. Sci. Eng.* **2019**, *5*, 4463-4473.
[47] A. Ghose, M. Rebarz, O. V. Maltsev, L. Hintermann, C. Ruckebusch, E. Fron, J. Hofkens, Y. Mély, P. Naumov, M. Sliwa, P. Didier, 'Emission Properties of Oxyluciferin and Its Derivatives in Water: Revealing the Nature of the Emissive Species in Firefly Bioluminescence', *J. Phys. Chem. B* **2015**, *119*, 2638–2649.
[48] M. Wendel, S. Nizinski, D. Tuwalska, K. Starzak, D. Szot, D. Prukala, M. Sikorski, S. Wybraniec, G. Burdzinski, 'Time-resolved spectroscopy of the singlet excited state of betanin in aqueous and alcoholic solutions' *Phys. Chem. Chem. Phys.* **2015**, *17*, 18152–18158.